Electron Optics Lectures

Chris E. Royatt

April-May 1967

Very Tentative Outline

1. Introduction
   Subjects to be Covered
   References
   Basic Relations
   "Index of Refraction"
   Helmholz-Lagrange Law
   Conservation of Richtstrahlwert
   Langmuir's Equation
2. Thick Lens Equations
   Calculations with Thick Lenses
   Matrix Methods
   Systems of Simple Lenses
   One-stage deceleration
   Variable ratio lens
3. Windows and Pupils
   Field Lens
   Computer Program
4. Diode Properties
   Design of Low Voltage Guns with Diode Source
   Space Charge Limits on Beams
5. Properties of Spherical Deflector
   Space Charge in Spherical Deflector
   Optimization of Monochromator

Electron Optics Lectures

April-May 1967

6. Realization of Optimum Monochromator
   - Design of Input and Output Optics

7. Scattering Geometries
   - Optimization of Energy Analyzer

8. Special Systems
   - Futrell Ion Lens
   - Brehm System for Photodetachment
   - IBM System for Photoionization

Electron Optics Books

V.E. Coslett, Introduction to Electron Optics, Oxford, 1946.

K.R. Spangenberg, Vacuum Tubes, Mc-Graw Hill, New York, 1948.

J.R. Pierce, Theory and Design of Electron Beams, 2nd Edition, D. Van Nostrand, Princeton N.J, 1954.

P. Grivet, Electron Optics, Pergamon, Oxford, 1965.

O. Klemperer, Electron Optics, 2nd Edition, Cambridge, 1953.

L.M. Myers, Electron Optics, D. Van Nostrand, New York, 1939.

V.K. Zworykin, G.A. Morton, E.G. Ramberg, J. Hillier, and A.V. Vance, Electron Optics and the Electron Microscope, John Wiley and Sons, New York, 1945.

P.A. Sturrock, Static and Dynamic Electron Optics, Cambridge, 1955.

W. Glaser, Grundlagen der Elektronenoptik, Springer, 1952.

Electron Physics Section Papers

J.A. Simpson, "Design of Retarding Field Analyzers", Rev. Sci. Instr. 32, 1283 (1961)

J.A. Simpson and C.E. Kuyatt, "Limitations on Electron Beam Density of Unipotential Electron Guns at Low Voltages", J. Research NBS 67C, 279 (1963).

J.A. Simpson and C.E. Kuyatt, "Design of Low Voltage Electron Guns", Rev. Sci. Instr. 34, 265 (1963)

J.A. Simpson and C.E. Kuyatt, "Anomalous Energy Spreads in Electron Beams", Jour. Appl. Phys. 37, 3805 (1966)

C.E. Kuyatt and J.A. Simpson, "Electron Monochromator Design", Rev. Sci. Instr. 38, 103-111 (Jan. 1967)

C.E. Kuyatt, "Measurement of Electron Scattering from a Static Gas Target", to be published in Methods of Experimental Physics, ed. L. Marton, Vol. 8.

J.A. Simpson, "High Resolution, Low Energy Electron Spectrometer", Rev. Sci. Instr. 35, 1698 (1964)

Electron Optics Lectures

Chris L. Koyalt

LECTURE 1.

April 4, 1967

Introduction
Subjects to be Covered
References
Basic Relations
"Index of Refraction"
Helmholz – Lagrange Law
Abbe Sine Law
Conservation of Richtstrahlwert
Langmuir's Equation
Normal and Total Energy Distributions
Beam and Pencil Angles
r-θ Diagrams

Electron Optics Lectures

April 4, 1967

Lecture I

ATTENDANCE SHEET (who wants notes, notices)
BRING BOOKS AND REPRINTS
TIME FOR NEXT LECTURE - 10:00?

Introduction

The purpose of this series of lectures is to set forth in some detail the principles and methods of electron optics which are needed to design guns, monochromators, and energy analyzers of optimum and predictable performance. The low energy region, less than a few hundred eV, will be emphasized, but the general principles can have application at higher energies.

In order to reduce the time required to a manageable length, no attempt will be made to rigorously derive the basic equations. These equations will be assumed, with references to sources for those interested in derivations, and their application to electron optical design will be given in some detail.

Nearly everything I'm going to talk about I learned after joining NBS in 1960, and much of it benefitted greatly through discussions and collaboration with John Simpson.

It was a surprise to me, after joining NBS, to find that there existed very little solid information on the design of low voltage electron guns, high resolution, high current electron monochromators, or variable ratio lenses. We are now in a position to design all of these devices, with some degree of confidence that they will operate as desired. However, many interesting and difficult problems remain, such as the accurate calculation of lens properties including aberrations, the development of higher f number monochromators, and the production of millivolt energy width beams.

"Index of Refraction"

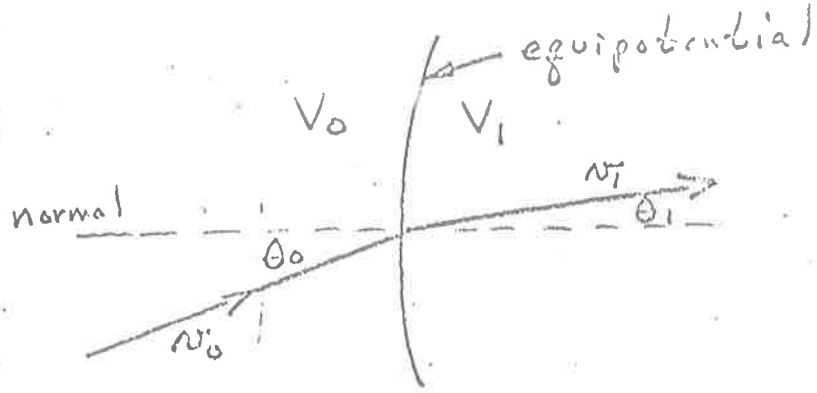

Tangential component of velocity is unchanged. Hence

$$v_0 \sin\theta_0 = v_1 \sin\theta_1$$

From conservation of energy:

$$eV_0 = \tfrac{1}{2} m v_0^2 \qquad eV_1 = \tfrac{1}{2} m v_1^2 \longrightarrow \frac{v_1}{v_0} = \sqrt{\frac{V_1}{V_0}}$$

Giving

$$\frac{\sin\theta_0}{\sin\theta_1} = \frac{v_1}{v_0} = \sqrt{\frac{V_1}{V_0}} = \frac{N_1}{N_0}$$

Where N_1, N_0 may be thought of as the "refractive indices". Hence $\sqrt{V}$ may be used as a refractive index, with $V=0$ when electrons are at rest.

Law of Helmholtz and Lagrange

Along any electron beam path where current is conserved and there are no energy dispersing devices: (No imaging assumed)

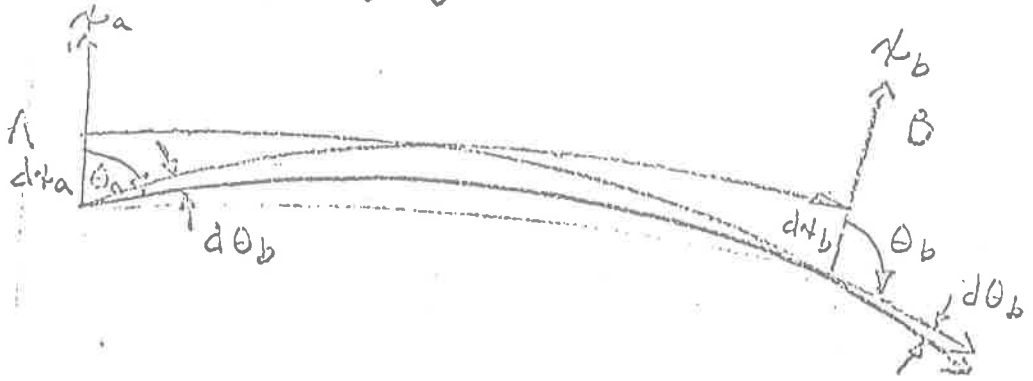

STURROCK

$$\sqrt{E_a}\sin\theta_a\, d\theta_a\, dx_a = -\sqrt{E_b}\sin\theta_b\, d\theta_b\, dx_b \qquad \text{EXACT}$$

If $\theta_a = 90°$, $\theta_b = 90°$, then

$$\sqrt{E_a}\, d\theta_a\, dx_a = -\sqrt{E_b}\, d\theta_b\, dx_b \qquad \text{EXACT}$$

Note: dx_a, dx_b perpendicular to path.

Applying this relation in a perpendicular direction, and multiplying:

$$E_a\, d\Omega_a\, dA_a = E_b\, d\Omega_b\, dA_b \qquad \text{EXACT}$$

$d\Omega$ = solid angle (θ^2)

dA = area, perpendicular to path

All these are differential relations.

Now assume imaging between A and B:

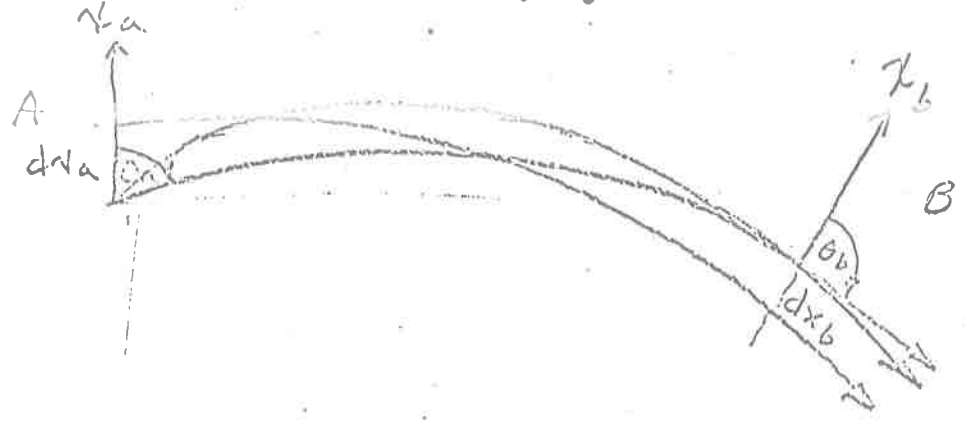

$$\sqrt{E_a}\,\sin\theta_a\,d\theta_a\,dx_b = \sqrt{E_b}\,\sin\theta_b\,d\theta_b\,dx_b \qquad \text{EXACT}$$

If $\theta_a = \theta_b = 90°$, and $M = \dfrac{dx_b}{dx_a}$, then

$$\boxed{\sqrt{E_a}\,d\theta_a = M\sqrt{E_b}\,d\theta_b} \quad (A) \qquad \text{EXACT}$$

Suppose θ_a and θ_b not $\perp$ to A and B.

Define new θ_a and θ_b : (π minus previous θ's)

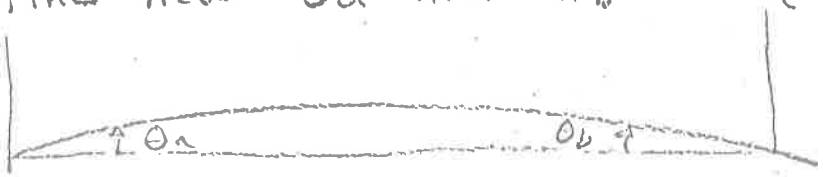

Then $\sqrt{E_a}\cos\theta_a\,d\theta_a = M\sqrt{E_b}\cos\theta_b\,d\theta_b$

Since $\cos 18° \cong 0.95$, $\cos 12° \cong 0.98$, this form will be needed only for very accurate work and large angles.

Integral Form

Integrate last equation from 0 to θ_a, and 0 to θ_b:

Assume M does not depend on θ_a.

$$\boxed{-\sqrt{E_a}\sin\theta_a = M\sqrt{E_b}\sin\theta_b} \quad (B)$$

This is the Abbe-Helmholtz Sine Law.

Again, for all but the most accurate work, ($\sin\theta = \theta$ to 2% at 20°, 5° at 29°)

$$-\sqrt{E_a}\,\theta_a = M\sqrt{E_b}\,\theta_b$$

Note — When the more accurate forms are required they must be applied as a function of image position, since the central ray angles will vary across the image. In this case it is better to visualize the situation in terms of windows and pupils, which will be taken up later.

Richtstrahlwert ("brightness", current intensity)

$$R = \frac{dI}{dA\, d\Omega}$$

Then conservation of current, together with

$$E_a\, d\Omega_a\, dA_a = E_b\, d\Omega_b\, dA_b$$

gives $$\frac{dI}{E_a\, d\Omega_a dA_a} = \frac{dI}{E_b\, d\Omega_b dA_b}$$

Or $$\frac{R_a}{E_a} = \frac{R_b}{E_b}$$

So Richtstrahlwert divided by the energy is a conserved quantity.

Langmuir's Equation

Because of the thermal energy spread of electrons emitted from a thermionic cathode, a limit is placed on the maximum current density which can be produced in an electron beam:

By applying the Helmholtz-Lagrange Law between the cathode and plane 2, and integrating over the energy distribution:

$$J_2^{max} = J_{cathode}\left[1 + \frac{E_2}{kT}\right]\sin^2\theta_2$$

J = current density

k ≅ 11,600 eV/°K

The term "1" can be neglected when E_2 is larger than a few electron-volts.

The maximum value of J_2 is achieved only when the current transmission efficiency goes to zero. In practice, the maximum value can be closely approached.

Although the full derivation of the Langmuir Eq. is involved, an approximate form restricted to an image plane can be derived from the Abbe sine law:

M = magnification from cathode to image

Then $J_2 = \frac{1}{M^2} J_{cathode}$

The Abbe sine law gives

$$M^2 = \frac{E_1 \sin^2\theta_1}{(E_2 + kT)\sin^2\theta_2}$$

Take $E_1 = kT$, $\sin\theta_1 = 1$,

$$J_2 = J_{cathode}\left(\frac{E_2 + kT}{kT}\right)\sin^2\theta_2 .$$

Total Energy Distribution from Cathode:

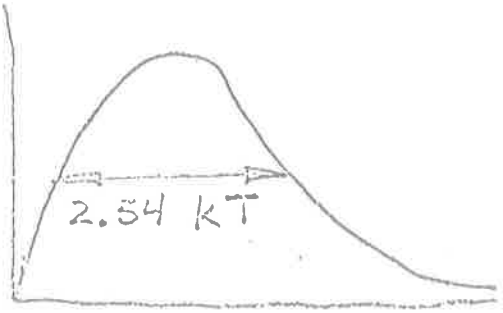

Normal Energy Distribution from Cathode:

? Normal component of all electrons or electrons emitted normally ?

Characterization of Angles in a Beam

Pencils form the image:

Centers of pencils form Beam Angle:

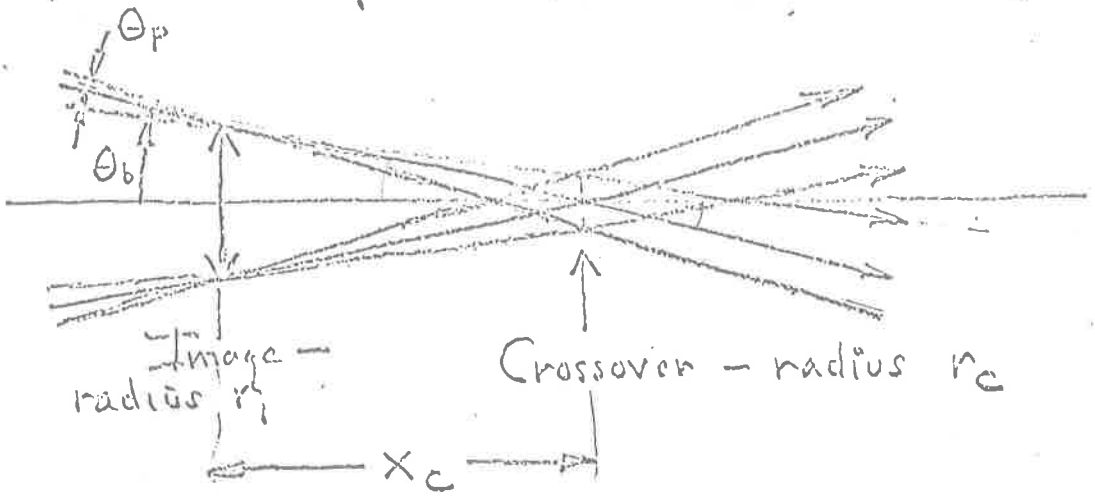

θ_p = pencil half-angle (≡ beam angle at crossover)

θ_b = beam angle (≡ pencil angle at crossover)

IMAGE ⟷ WINDOW

CROSSOVER ⟷ PUPIL

R–θ Diagram

First, consider an image with cross-over at infinity. (Zero beam angle)

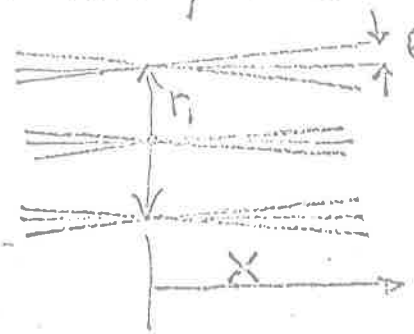

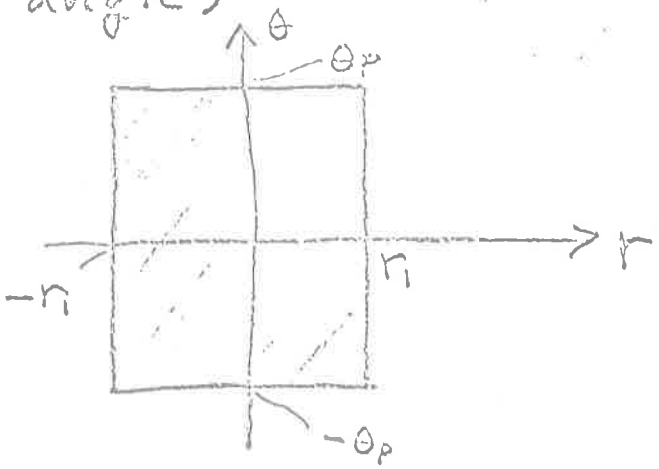

Now look at distance x to right of image. Rays of constant angle are same distance apart, but displaced in r by $x\theta$.

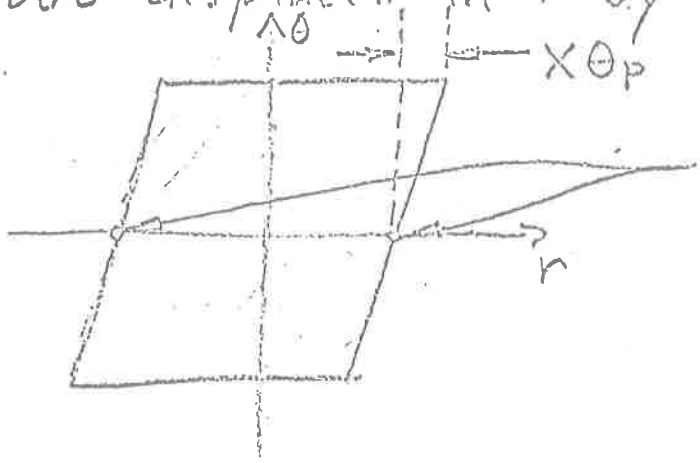

After a long distance:

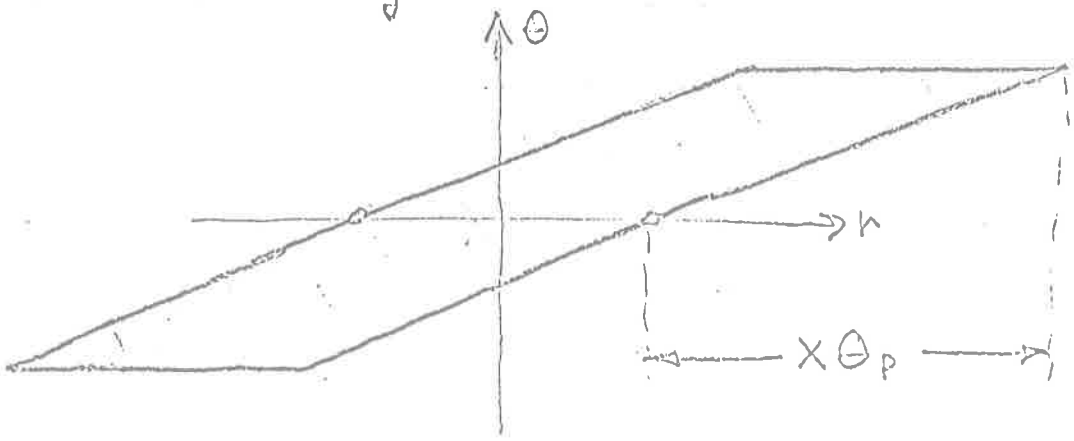

Note that area remains constant — A sort of integral form of the Helmholtz-Lagrange law.

Differential form of H-L says that a differential of area in r-θ space remains constant.

Now draw r–θ diagram for top of p. (17)

Note first that

$$r_i = x_c \theta_b \qquad r_c = x_c \theta_p$$

$$\Rightarrow \frac{r_i}{r_c} = \frac{\theta_b}{\theta_p} \Rightarrow r_i \theta_p = r_c \theta_b$$

Same as applying H–L between image and crossover.

AT IMAGE

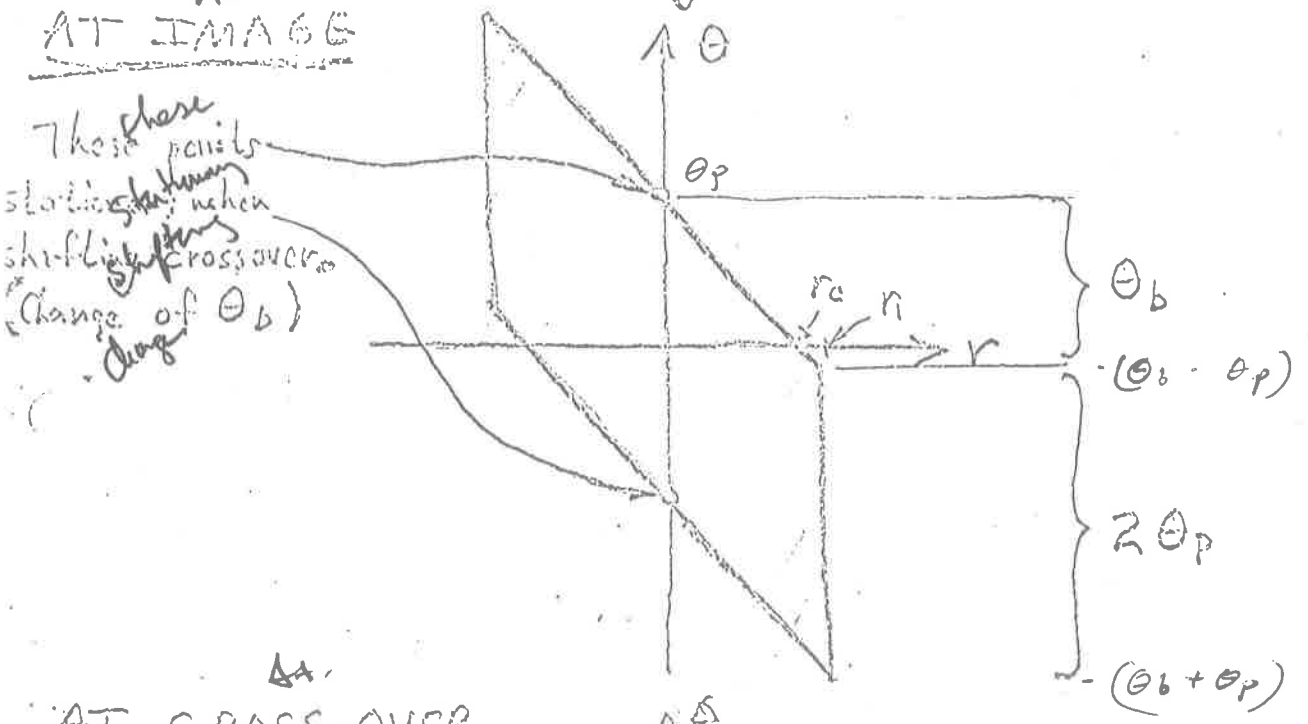

AT CROSS-OVER

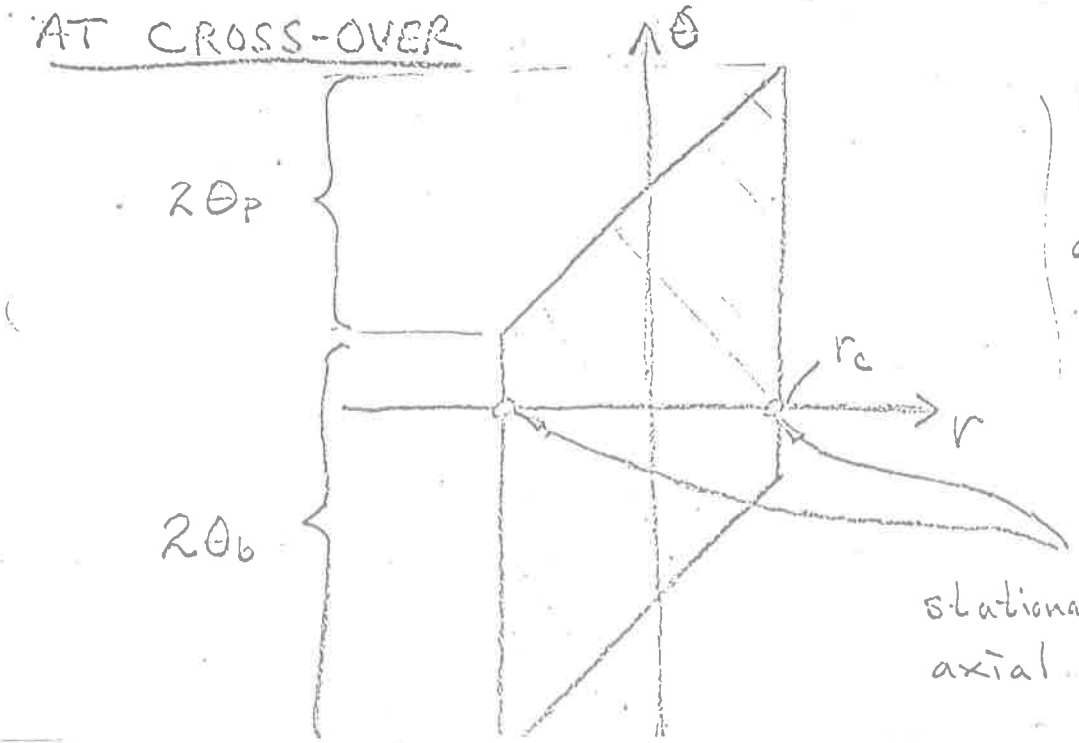

Note that all areas are the same.

Electron Optics Lectures

Chris E. Kayatt

April 18, 1967

Lecture 2

- Electrostatic Lenses
  - Two-Cylinder
  - Aperture-Cylinder
  - Two-Aperture
  - Calbick
  - Einzel
- Thick Lens Equations (Gaussian Optics)
  - Newtonian Form
  - $\frac{1}{f}$ Form.
  - Helmholz-Lagrange Law.
  - Magnification
- F_1, F_2, f_1, f_2 Curves
- P, Q Curves
- Lens Calculation Methods
  - P, Q Curves
  - f_1, f_2, F_1, F_2 Curves
  - Matrix Method
    - Example

Electron Optics Lectures

Chris E. Kuyatt

Lecture 2.

April 18, 1967

Electrostatic Lenses

Two-Cylinder

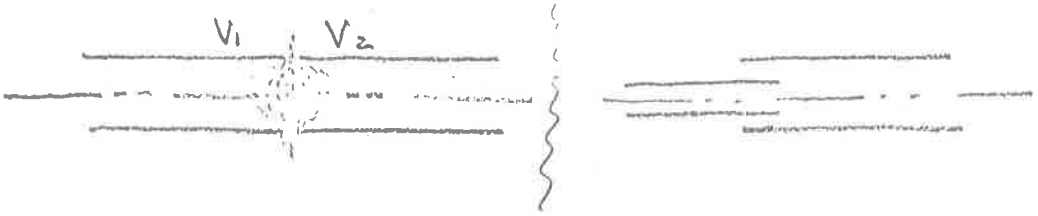

Aperture-Cylinder

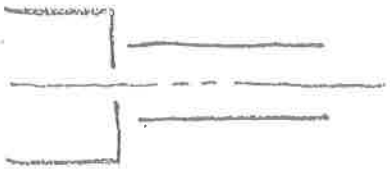

Two-Aperture

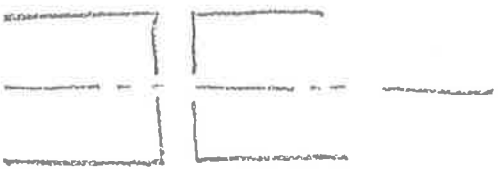

"Calbick" Lens (Uniform Fields $\mathcal{E}_1$, $\mathcal{E}_2$)

converging $\mathcal{E}_2 > \mathcal{E}_1$

diverging $\mathcal{E}_2 < \mathcal{E}_1$

"Einzel" (Symmetrical, Univoltage) Lens

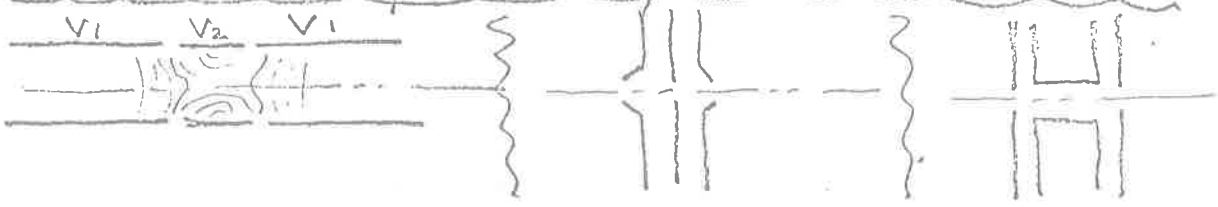

Thick Lens Equations (Gaussian Optics)

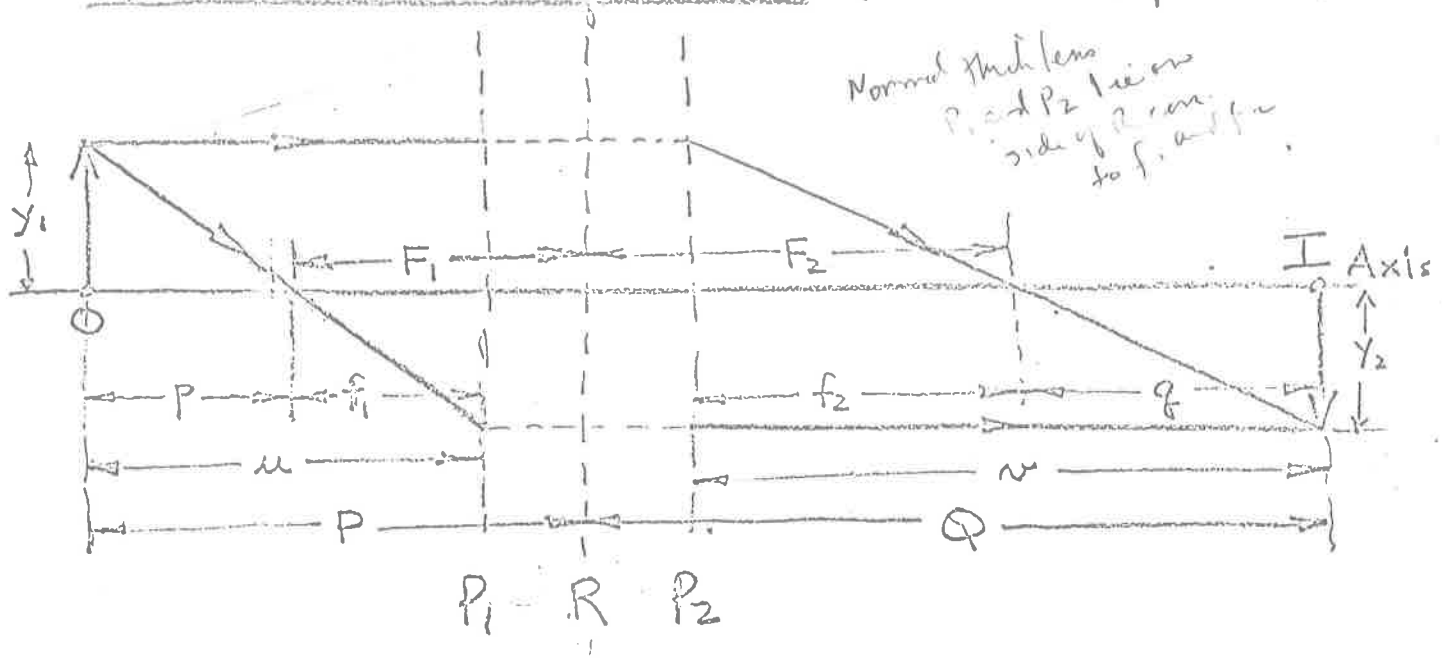

R: midplane or reference plane

P_1: object principle plane

P_2: image principle plane

F_1, F_2: distances of focal points from R

f_1, f_2: focal lengths

NOTE: In real life, P_1 and P_2 are crossed and on the low voltage side of the lens.

Newtonian Lens Equation

M = lateral magnification

$$M = \frac{y_2}{y_1} = -\frac{f_1}{p} = -\frac{q}{f_2}$$

So $$\boxed{f_1 f_2 = pq}$$

Most convenient to use in practice.

the "second principal ray." For lenses with initial and final gradients of potential that are zero the initial and final portions of the rays will be straight lines. The principal rays of an equal-diameter two-cylinder lens are shown in Fig. 13.20. Any general ray may be expressed as a combination of these two rays.

As mentioned before, the left portion of a lens such as that of Fig. 13.20 has a convergent action, while the right portion has divergent action. The strength of these two portions is such that the convergent action always dominates. The first principal ray, taken as moving from right to left, first experiences divergent action and then a stronger

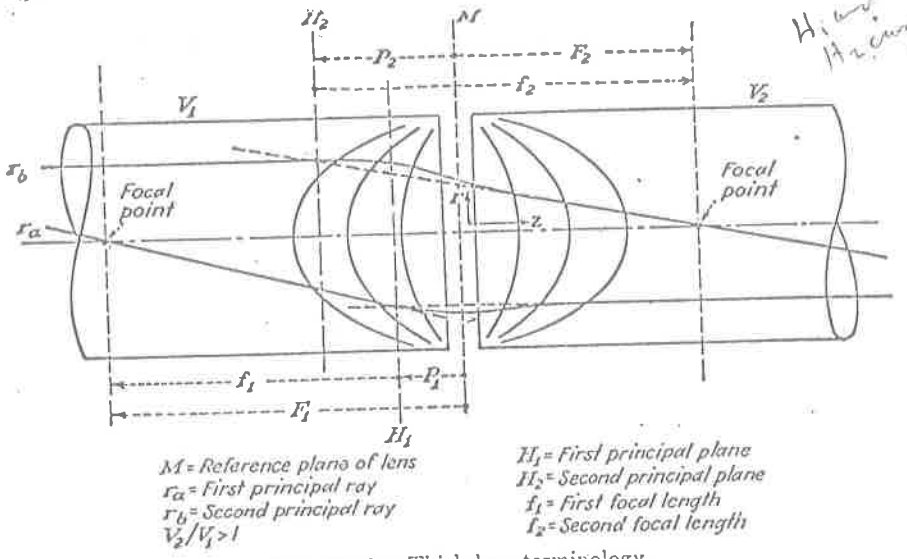

FIG. 13.20.—Thick-lens terminology.

convergent action. The second principal ray, taken as moving from left to right, first experiences a convergent action and then a weaker divergent action.

The principal rays serve to define the four thick-lens parameters. *If the initial and final straight-line portions of the principal rays are extended until they intersect, the intersections locate what are known as the "principal planes."* The principal planes are shown as H_1 and H_2 in Fig. 13.20. The location of the principal planes relative to the reference plane, usually the midplane or electrode junction, is given by the distances P_1 and P_2. Almost without exception, the relative location of the principal planes is as shown in Fig. 13.20. Both principal planes lie on the foreside of the lens. Furthermore, the principal planes are crossed, *i.e.*, the second principal plane lies before the first principal plane. Although this is

In terms of u and v:

$$\frac{u}{f_1} = \frac{v}{q} \Rightarrow \frac{u}{v} = \frac{f_1}{q} = \frac{p}{f_2} = \frac{u - f_1}{f_2}$$

So $$\frac{u}{v} = \frac{u - f_1}{f_2} \Rightarrow \frac{f_2}{v} = \frac{u - f_1}{u} = 1 - \frac{f_1}{u}$$

And $$\boxed{\frac{f_1}{u} + \frac{f_2}{v} = 1}$$ Less convenient to use.

Helmholtz-Lagrange Law

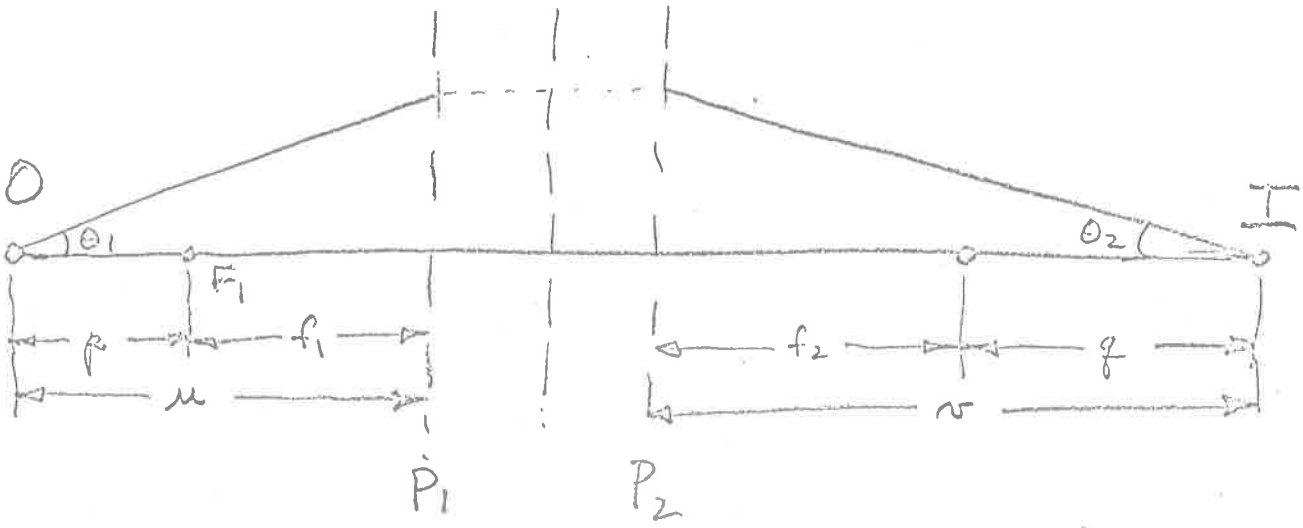

$$\frac{\tan\theta_2}{\tan\theta_1} = -\frac{u}{v} = -\frac{p}{f_2} = -\frac{f_1}{q}$$

For paraxial rays, it can be shown that

$$\frac{f_1}{f_2} = \sqrt{\frac{V_1}{V_2}}$$

If one focal length is known, the other can be calculated.

Now $\frac{f_1}{f_2} = \frac{f_1}{p} \times \frac{p}{f_2} = \frac{y_2}{y_1} \frac{\tan\theta_2}{\tan\theta_1}$

So $\sqrt{\frac{V_1}{V_2}} = \frac{y_2}{y_1} \frac{\tan\theta_2}{\tan\theta_1}$

Put $M = \frac{y_2}{y_1}$

$$\sqrt{V_1}\tan\theta_1 = M\sqrt{V_2}\tan\theta_2$$

This would be the Abbe-Helmholz Sine law, if tan was replaced by sin. However, for paraxial rays, $\tan\theta \cong \sin\theta$ { to .2% at 12° ; to 5% at 18°

so that the deviations will not be important under ordinary conditions with small angles.

It does illustrate the fact that the principle planes and focal points of a lens are fixed only for paraxial rays.

So, for <u>small angles</u>:

$$\sqrt{V_1}\,\theta_1 = M\sqrt{V_2}\,\theta_2$$

Let m = angular magnification $= \frac{\theta_2}{\theta_1}$

$$\boxed{m M = \sqrt{\frac{V_1}{V_2}}} \quad \text{and} \quad \boxed{m = \frac{u}{v} = -\frac{p}{f_2} = -\frac{f_1}{q}}$$

decrease lateral magnification, angular mag. must increase

increase voltage ratio, angular magnification must decrease (if one accelerating).

Also $$\boxed{M = \frac{1}{m}\sqrt{\frac{V_1}{V_2}} = \frac{n}{m}\sqrt{\frac{V_1}{V_2}}}$$

To procede with lens calculations using these thick lens equations, one needs data on f_1, f_2, F_1, F_2 for a variety of lens configurations, and for a range of electrode potentials. Some of this data can be found in the books cited, and in widely scattered papers. The most extensive set of data is to be found in Spangenberg's book. This data is probably accurate to about 10 to 20% over most of its range, and has been used in much of our design work.

In Spangenberg, pp. 369 – 373, are shown f_1, f_2, F_1, F_2 for cylinder and aperture lenses of several configurations. One of these pages I show here for cylinder lenses. Contrary to the practice of Spangenberg, I will treat all of the quantities f_1, f_2, F_1, F_2 as positive quantities, with object quantities measured positive to the left, and image properties measured positive to the right.

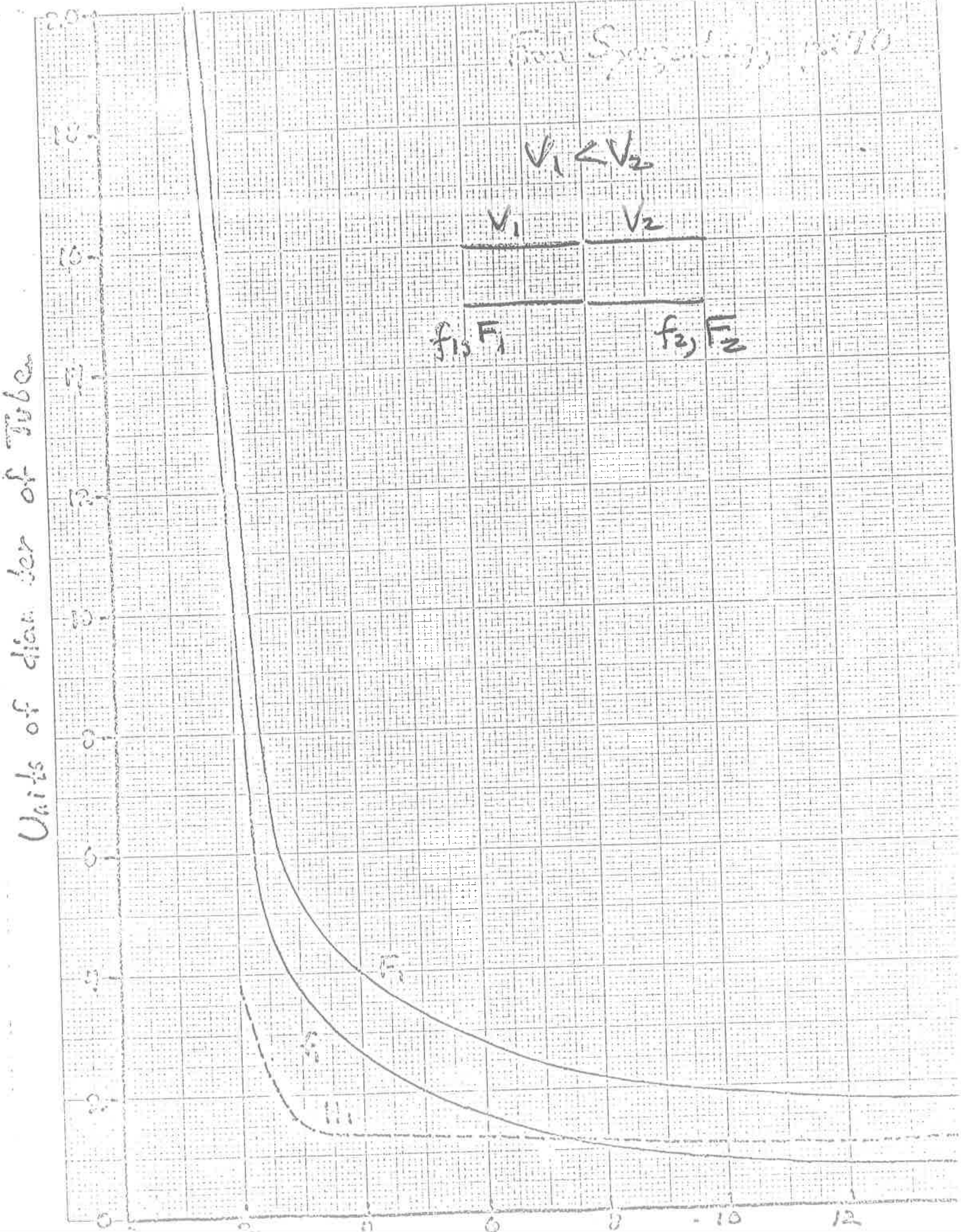

$V_1 < V_2$
V_1
V_2
f_1, F_1
f_2, F_2
Units of dia. of tube
F_1
10
12

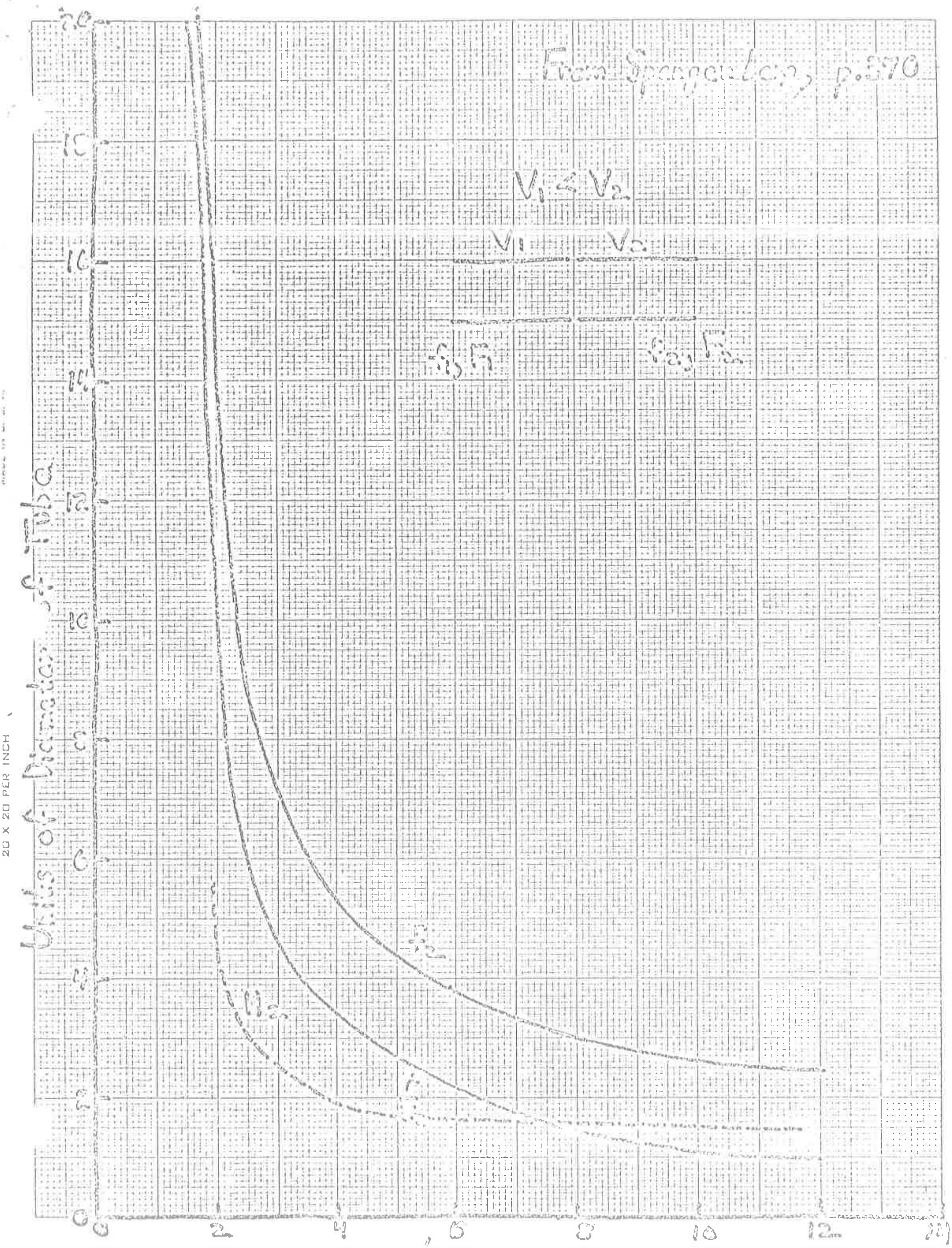
From Spangenberg, p.370
V1 < V2
V1
V2
Units of Diameter of Tube
20 X 20 PER INCH
0
2
4
6
8
10
12
14

P, Q Curves

For more convenient use, Spangenberg has converted the f_1, f_2, F_1, F_2 curves to curves of image and object distance, with magnification as a parameter. One of these pages, for cylinder lenses, is reproduced here. These P, Q curves are very convenient for design work when the image and object are real. When virtual images or objects are involved, the focal properties will need to be used, or P, Q curves for virtual images and objects could be derived from the focal properties.

For accelerating lenses, $M \cong 0.8 \frac{Q}{P}$.

Lens Calculation Methods

1) P, Q Curves
2) f_1, f_2, F_1, F_2 curves
3) Matrix methods
4) Computer Program

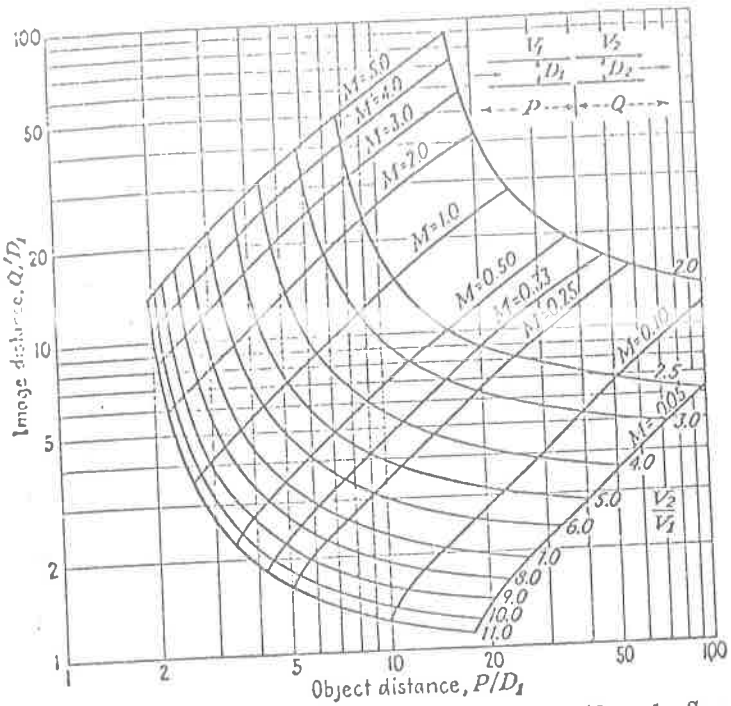

FIG. 13.38.—P-Q curves of a two-cylinder lens, $D_2/D_1 = 1$, $S = 0.1D_1$.

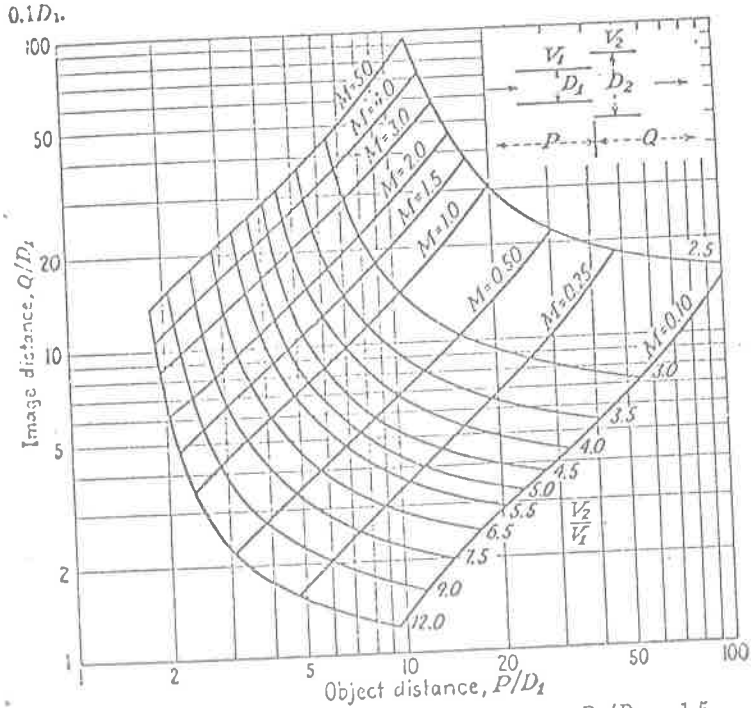

FIG. 13.39.—P-Q curves of a two-cylinder lens, $D_2/D_1 = 1.5$.

Calculations with f_1, f_2, F_1, F_2 curves.

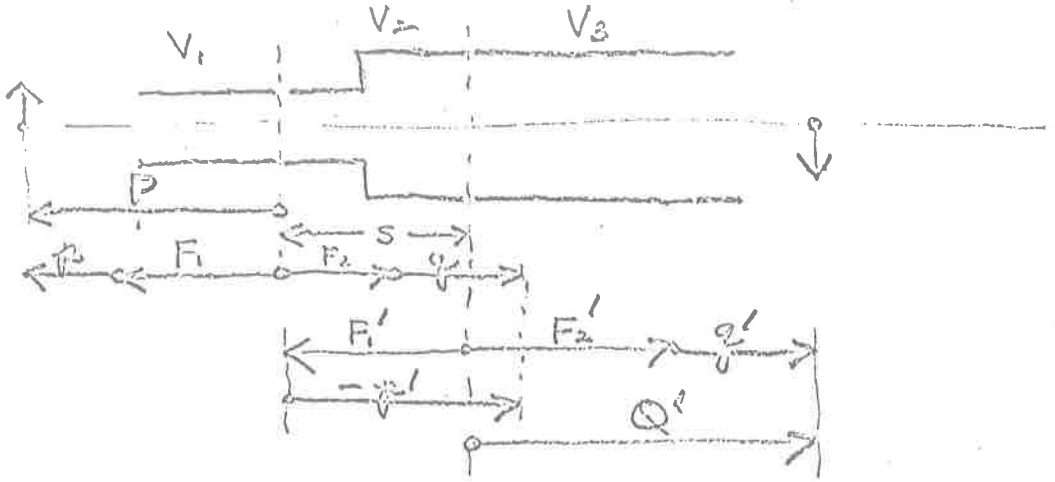

$$p = P - F_1 \qquad q = \frac{f_1 f_2}{p} \qquad M_{12} = -\frac{f_1}{p} = -\frac{q}{f_2}$$

$$-p' = q + F_2 - s + F_1' \qquad q' = \frac{f_1' f_2'}{p'} \qquad M_{23} = -\frac{f_1}{p'} = -\frac{q'}{f_2}$$

$$Q' = q' + F_2'$$

From $\frac{V_2}{V_1}$ and $\frac{V_3}{V_2}$, the f's and F's are found from Spangenberg's curves, then multiplied by the diameter of the lenses to get actual values. Then set up a tabular list of the quantities to be calculated and proceed.

I find that an equivalent procedure using matrices is more convenient in practice.

Matrix Method

Let an electon be represented by a vector:

$$\begin{pmatrix} \text{radius} \\ \text{slope} \end{pmatrix}$$

Then a linear displacement ΔZ in field--free space is found by operating on this vector with the matrix:

$$\begin{pmatrix} 1 & \Delta Z \\ 0 & 1 \end{pmatrix}\begin{pmatrix} \text{radius} \\ \text{slope} \end{pmatrix} = \begin{pmatrix} \text{position} + \Delta z(\text{slope}) \\ \text{slope} \end{pmatrix}$$

The electron ray retains its slope.

The matrix operating between the principle planes of a lens is:

$$\begin{pmatrix} 1 & 0 \\ -\frac{1}{f_2} & \frac{f_1}{f_2} \end{pmatrix}$$

To demonstrate that this is the correct matrix, apply it to a lens!

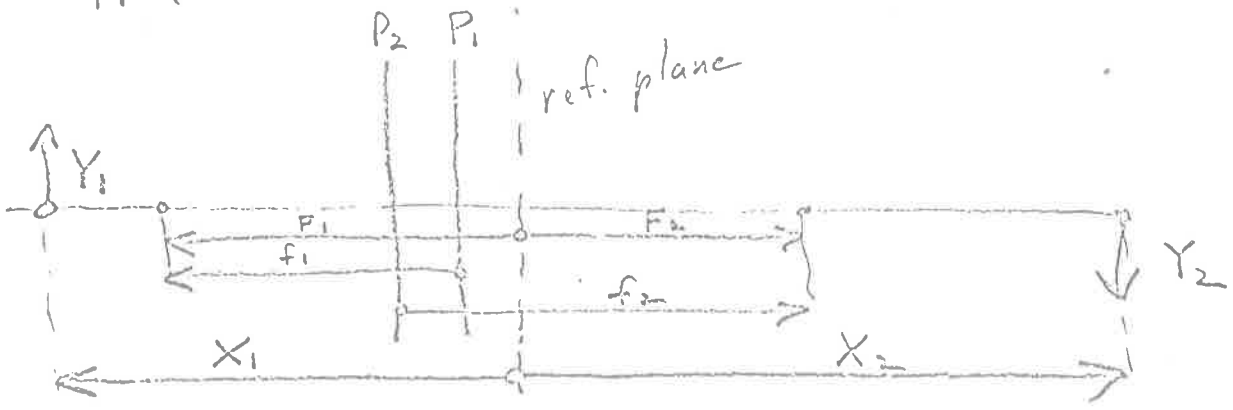

Linear translation to P_1:

$$\mathcal{M}_1 = \begin{pmatrix} 1 & X_1 - F_1 + f_1 \\ 0 & 1 \end{pmatrix}$$

Between Principle Planes

$$\mathcal{M}_2 = \begin{pmatrix} 1 & 0 \\ -\frac{1}{f_2} & \frac{f_1}{f_2} \end{pmatrix}$$

Linear translation from P_2 to X_2:

$$\mathcal{M}_3 = \begin{pmatrix} 1 & X_2 - F_2 + f_1 \\ 0 & 1 \end{pmatrix}$$

Then

$$\begin{pmatrix} Y_2 \\ Y_2' \end{pmatrix} = \mathcal{M}_3 \mathcal{M}_2 \mathcal{M}_1 \begin{pmatrix} Y_1 \\ Y_1' \end{pmatrix}$$

$$\mathcal{M}_3 \mathcal{M}_2 \mathcal{M}_1 = \begin{pmatrix} 1 & X_2 - F_2 + f_2 \\ 0 & 1 \end{pmatrix} \begin{pmatrix} 1 & 0 \\ -\frac{1}{f_2} & \frac{f_1}{f_2} \end{pmatrix} \begin{pmatrix} 1 & X_1 - F_1 + f_1 \\ 0 & 1 \end{pmatrix}$$

$$= \begin{pmatrix} 1 & X_2 - F_2 + f_2 \\ 0 & 1 \end{pmatrix} \begin{pmatrix} 1 & X_1 - F_1 + f_1 \\ -\frac{1}{f_2} & -\frac{X_1 - F_1}{f_2} \end{pmatrix}$$

$$= \begin{pmatrix} -\frac{X_2 - F_2}{f_2} & X_1 - F_1 + f_1 - \left(\frac{X_1 - F_1}{f_2}\right)(X_2 - F_2 + f_2) \\ -\frac{1}{f_2} & -\frac{X_1 - F_1}{f_2} \end{pmatrix}$$

Take out $-\frac{1}{f_2}$:

$$= -\frac{1}{f_2} \begin{pmatrix} X_2 - F_2 & (X_1 - F_1)(X_2 - F_2) - f_1 f_2 \\ 1 & X_1 - F_1 \end{pmatrix}$$

As a check, note that determinant is $\frac{f_1 f_2}{f_2^2} = \frac{f_1}{f_2}$.
(Coefficient in front must be squared when taking the determinant)

In general, the matrix coefficients have the meaning:

$$\begin{pmatrix} \dfrac{\text{linear magnification}}{\text{input distance, parallel ray}} & \dfrac{\text{distance out}}{\text{input angle}} \\ \dfrac{\text{angle out}}{\text{input distance, parallel ray}} & \text{angular magnification} \end{pmatrix}$$

Hence condition for imaging is that

$$(X_1 - F_1)(X_2 - F_2) - f_1 f_2 = 0$$

$$X_2 - F_2 = \frac{f_1 f_2}{X_1 - F_1} \longrightarrow X_2 = F_2 + \frac{f_1 f_2}{X_1 - F_1}$$

$$M_{12} = -\frac{X_2 - F_2}{f_2} = -\frac{f_1}{X_1 - F_1}$$

$$m_{12} = -\frac{X_1 - F_1}{f_2} = -\frac{f_1}{X_2 - F_2}$$

} these agree with equations on p. (7).

I will now give a numerical example for a system of two tube lenses:

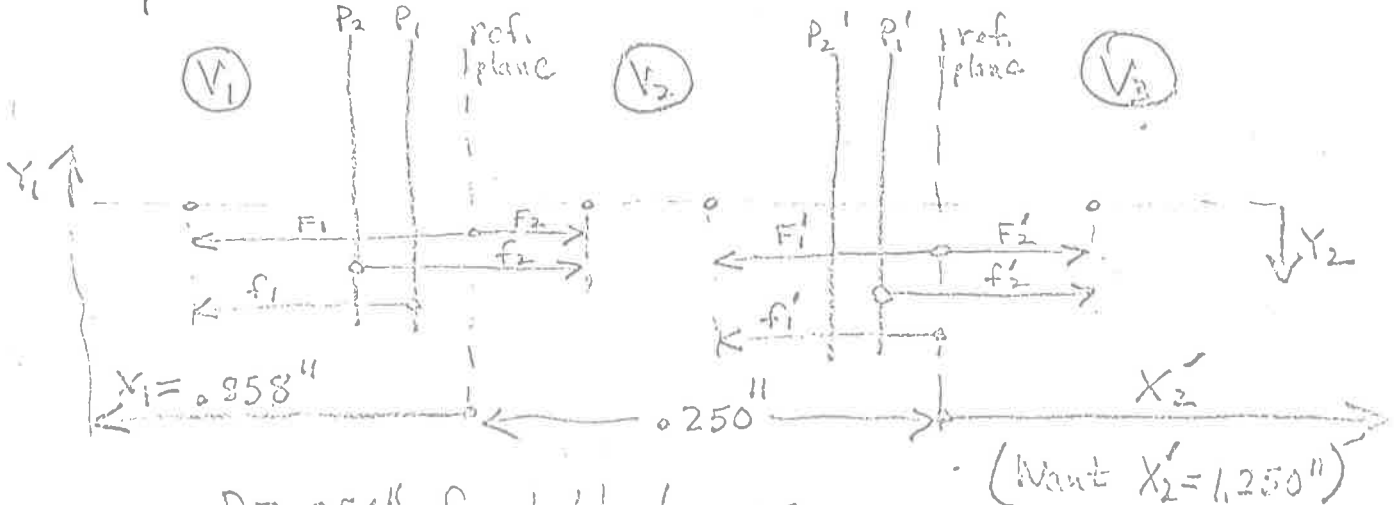

D = .250" for both lenses.

$V_1 = 70 \quad V_2 = 2.00 \quad V_3 = 400$

f_1/f_2

I: $\frac{200}{70} = 2.86 \quad f_1 = .982" \quad F_1 = 1.375" \quad f_2 = 1.880" \quad F_2 = 1.225" \quad .522$

II: $\frac{400}{200} = 2.0 \quad f_1' = 2.75" \quad F_1' = 3.70" \quad f_2' = 3.68" \quad F_2' = 2.50" \quad \times .748$

$.391$

Second lens

$$\mathcal{M}_{II} = -.272 \begin{pmatrix} X_2' - 2.50 & -3.70(X_2' - 2.50) - 10.12 \\ 1 & -3.70 \end{pmatrix}$$

NOTE: $\mathcal{M}_{tot} = \mathcal{M}_3 \mathcal{M}_2 \mathcal{M}_1$, $X_1 = .855$, $X_2 = .250$

$$= -.272 \begin{pmatrix} X_2' - 2.50 & -3.70X_2' + .88 \\ 1 & -3.70 \end{pmatrix}$$

NOTE! $\mathcal{M}_{II} = \mathcal{M}_3' \mathcal{M}_2' \mathcal{M}_1'$, $X_1' = 0$, $X_2' = X_2'$

First lens

$$\mathcal{M}_I = -.532 \begin{pmatrix} -.975 & (-.517)(-.975) - 1.846 \\ 1 & -.517 \end{pmatrix} = -.532 \begin{pmatrix} -.975 & -1.342 \\ 1 & -.517 \end{pmatrix}$$

$$\mathcal{M}_{II}\mathcal{M}_I = .1446 \left(\begin{array}{cc|c} -.975X_2' + 2.44 - 3.70X_2' - .88 & & -1.342X_2' + 3.35 + 1.913X_2' + .455 \\ -.975 & -3.70 & -1.342 + 1.913 \end{array}\right)$$

$$= .1446 \left(\begin{array}{cc|c} -4.68X_2' + 1.56 & & .581X_2' + 3.80 \\ -4.68 & & .581 \end{array}\right)$$

$$= \left(\begin{array}{cc|c} -.676X_2' + .226 & & .084X_2' + .549 \\ -.676 & & .084 \end{array}\right)$$

Check: Det. $= .019 + .371 = .390$

Image is at $X_2' = -\frac{.549}{.084} = -6.54 \quad M = 4.42 + .226 = 4.65$

At $X_2' = 1.250"$

$$\mathcal{M}_{II}\mathcal{M}_I = \begin{pmatrix} -.845 + .226 & .105 + .549 \\ -.676 & .084 \end{pmatrix} = \begin{pmatrix} -.619 & .654 \\ -.676 & .084 \end{pmatrix}$$

Check: $0_2 t_2 = -.052 + .442 = .390$

$$\begin{pmatrix} Y_1 \\ Y_1' \end{pmatrix} = \begin{pmatrix} 0 \\ .033 \end{pmatrix} \quad \begin{pmatrix} Y_2 \\ Y_2' \end{pmatrix} = \begin{pmatrix} .0216 \\ .00277 \end{pmatrix}$$

$$\begin{pmatrix} Y_1 \\ Y_1' \end{pmatrix} = \begin{pmatrix} .0335 \\ .033 \end{pmatrix} \quad \begin{pmatrix} Y_2 \\ Y_2' \end{pmatrix} = \begin{pmatrix} -.00402 + .0216 \\ -.00440 + .00277 \end{pmatrix} = \begin{pmatrix} .0176 \\ -.00163 \end{pmatrix}$$

$$\begin{pmatrix} Y_1 \\ Y_1' \end{pmatrix} = \begin{pmatrix} .0065 \\ -.033 \end{pmatrix} \quad \begin{pmatrix} Y_2 \\ Y_2' \end{pmatrix} = \begin{pmatrix} -.00402 - .0216 \\ -.00440 - .00277 \end{pmatrix} = \begin{pmatrix} -.0256 \\ -.00717 \end{pmatrix}$$

Beam is .0512" diam, Maximum angle is .00717 rad.

Other Matrices

Aperture Lens (Calbick Lens)

$$\begin{pmatrix} 1 & 0 \\ -\frac{(\mathcal{E}_2-\mathcal{E}_1)}{4V_0} & 1 \end{pmatrix}$$

$\frac{f_1}{f_2} = 1$

$-\frac{1}{f_2} = -\frac{\mathcal{E}_2-\mathcal{E}_1}{4V_0} \rightarrow f_2 = \frac{4V_0}{\mathcal{E}_2-\mathcal{E}_1}$

Uniform Field

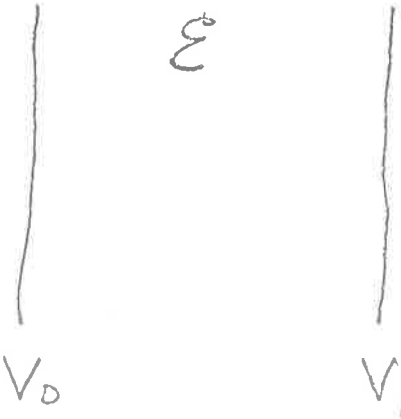

$$\begin{pmatrix} 1 & 2\frac{V_0}{\mathcal{E}}\left(\sqrt{\frac{V_1}{V_0}}-1\right) \\ 0 & \sqrt{\frac{V_0}{V_1}} \end{pmatrix}$$

Other Matrices

Aperture Lens (Calbick Lens)

$$\begin{pmatrix} 1 & 0 \\ -\frac{(\varepsilon_2-\varepsilon_1)}{4V_0} & 1 \end{pmatrix}$$

$\frac{f_1}{f_2} = -1$

$-\frac{1}{f_2} = -\frac{\varepsilon_2-\varepsilon_1}{4V_0} \rightarrow f_2 = \frac{4V_0}{\varepsilon_2-\varepsilon_1}$

Uniform Field

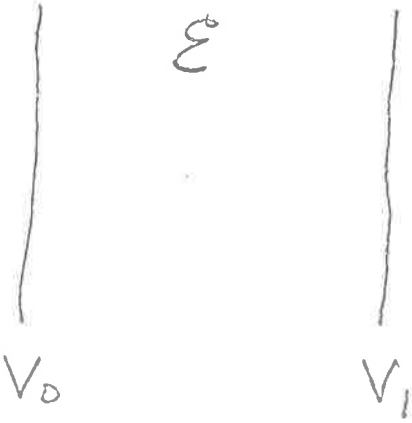

$$\begin{pmatrix} 1 & 2\frac{V_0}{\varepsilon}\left(\sqrt{\frac{V_1}{V_0}}-1\right) \\ 0 & \sqrt{\frac{V_0}{V_1}} \end{pmatrix}$$

Electron Optics Lectures

Lecture 3

Chris E. Kuyatt

May 2, 1967

Systems of Simple Lenses

One-stage Deceleration

Variable Ratio Lens

Combination of Two Simple Lenses

Einzel Lens as Special Case

Electron Optics Lectures

Lecture 3

Chris E. Kuyatt

May 2, 1967

SYSTEMS OF SIMPLE LENSES

One-Stage Decelerator

Design data:

Voltage Ratio	10:1
Magnification	1.5
Final diameter	.020"
Initial diameter	.013" ($\approx \frac{.020}{1.5}$)
Final pencil half-angle	.071 rad.
Final beam half-angle	0
Total length	$\approx$ 1.0"

These requirements resulted from analysis of the monochromator.

From Helmholz-Lagrange,

$$\text{Initial pencil half-angle} = \frac{.071}{\sqrt{10}}\,1.5 = .0336 \text{ rad.}$$

$\theta_1 = \frac{\theta_2}{\sqrt{V_2/V_1}}\,M \qquad \theta_2 = M\theta_1\sqrt{V_2/V_1}$

Plan to put angle and field stop on high-energy side of decelerator.

Make system as short as possible, with electron "filling factor" in lens $\leq 50\%$.

Requirement of zero "beam angle" requires angle aperture to be at first focal point of the lens.

Beam is expanding at rate of $\sim$.067"/inch, with initial size .013", so diameter at any distance x is

$$d = .013" + .067x$$

First find minimum lens diameter for an aperture lens, Spangenberg, p. 373.

$f_1 \cong 0.8\,D$ $F_1 = 3.4\,D$ (low voltage)

$V_2/V_1 = 10$ $f_2 \cong 2.6\,D$ $F_2 = 1.6\,D$ (high voltage)

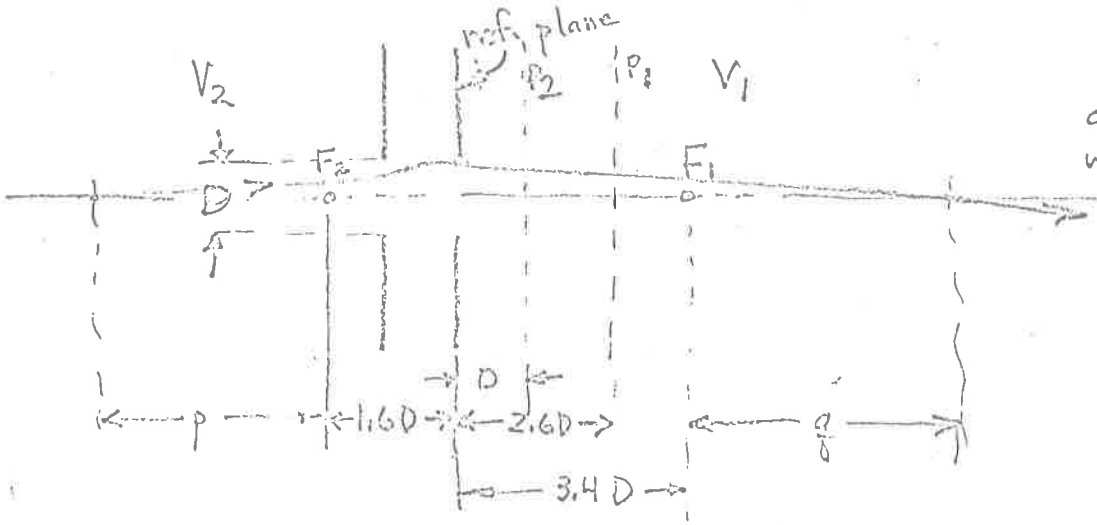

Note - This is one of the few lenses with principle planes not crossed.

Using thick lens equations:

$p = f_2 / M = 2.6\,D/1.5 = 1.73\,D$

$q = M f_1 = 1.5 \times 0.8\,D = 1.2\,D$

Overall length is: 7.93 D

Use projection from V_1 side to estimate beam size in the lens.

$$d \cong .020'' + 2(.071)5D = .020 + .71\,D$$

Note that filling factor is

$$\frac{d}{D} \cong .71 + \frac{.020}{D}$$

Even with a very large diameter lens the minimum filling factor is $> .71$.

Look for a lens with P_1 closer to the lens. Try the tube lens.

Tube lens, spacing = 0.1 D. Spangenberg, p. 370.

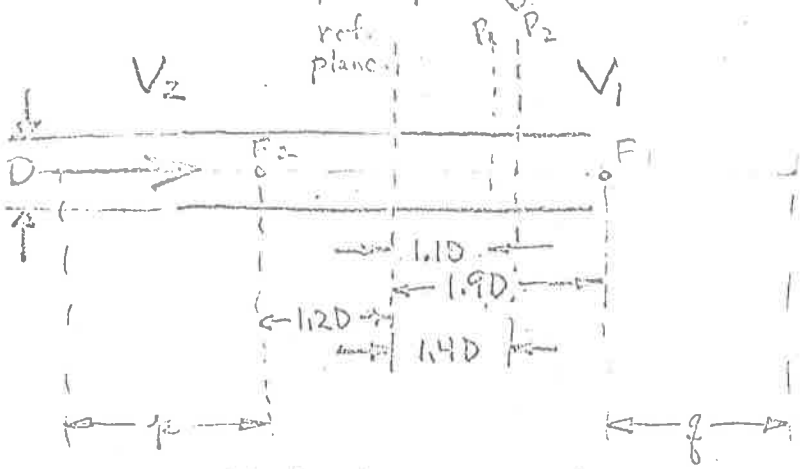

$V_2/V_1 = 10$

$f_1 = 0.8D \quad F_1 = 1.9D$

$f_2 = 2.6D \quad F_2 = 1.2D$

Using thick lens equations:

$p = f_2/M = 2.6D/1.5 = 1.73D$

$q = Mf_1 = 1.5 \times 0.8D = 1.2D$

Overall length is:

6.03 D

Use projection from V_1 side to estimate beam size in the lens.

$$d \cong .020'' + 2(3.1D)(.071) = .020 + .44D$$

Filling factor is

$$\frac{d}{D} = .44 + \frac{.02}{D} \Rightarrow$$

D = .5", d/D = .48
D = .2", d/D = .54
D = .1", d/D = .64

Note that the filling factors are smaller than for the aperture lens. According to Spangenberg curve, p. 392, $d/D \cong 0.5$ gives 1/3 the aberration than does $d/D \cong 0.8$. For $d/D \cong 0.5$, the minimum spot size is 1.5% of the tube diameter.

To give overall length of about 1"; $D \cong 0.16$".

Minimum spot size is about .0024", or a little over 10% of the final spot size.

The lens is now

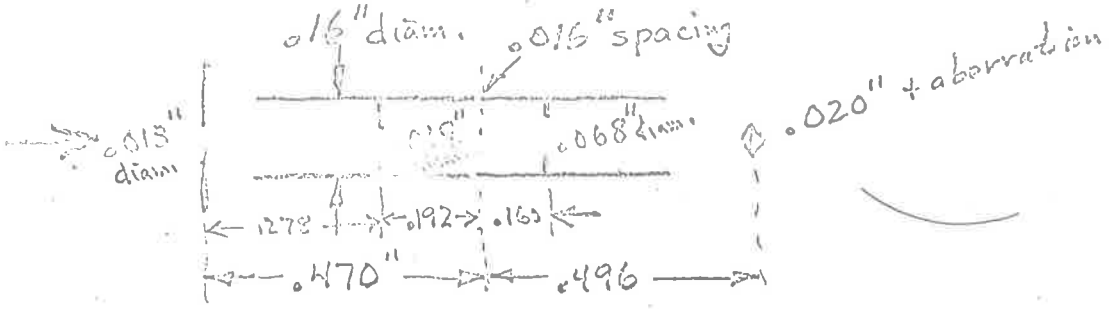

Size of aperture on left side:

$2 \times .278'' \times .0336 \text{ rad} = .0187''$ diam.

To screen out stray electrons scattered off wires and apertures, place a "spatter" aperture on the right side, one diameter from the center of the lens. This is .336" from the final image. Its size should be

$.020'' + 2(.091 \text{ rad.})(.336'') = .020'' + .048'' = .068''$ diam

If the .019" aperture were moved to the left, and adjusted appropriately in size, the pencils at the final image would become more and more converging. Such a beam might be useful in certain experimental arrangements

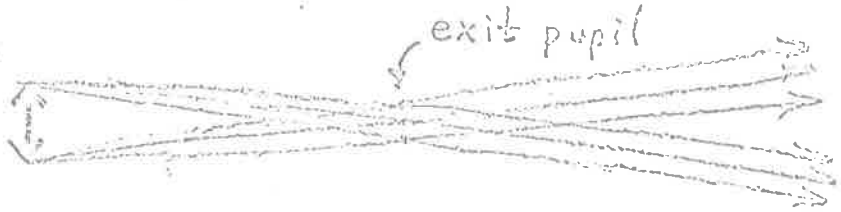

where a beam must be sent through two apertures. The exit pupil is the image of the angular aperture on the entrance side

Variable Ratio Lens

Incident Beam

Energy 70 and 25 eV
Size .013" diam.
Pencil half-angle .033 rad.
Beam half-angle ~0 rad.

Desired Beam

Position of image ~2.358"
Size of image .013" diam (unity magnification)
Energy Variable

To get started, suppose that the lens is composed of two closely spaced tube lenses. As a rough approximation, assume that the double lens has the same property as a single lens, namely

$$M \cong 0.8 \frac{Q}{P}$$

Q = image distance
P = object distance

for an accelerating lens.

For $M=1$, $P = 0.8\,Q$.

Total length is $P+Q = 1.8\,Q = 2.358$

So $Q = 1.31"$, $P = 1.048"$

From Spangenberg's P, Q curves it appears reasonable that the lens diameter be about ¼". ($P \sim 4D$, $Q \sim 5D$).

Apparatus constraints led us to modify this design to:

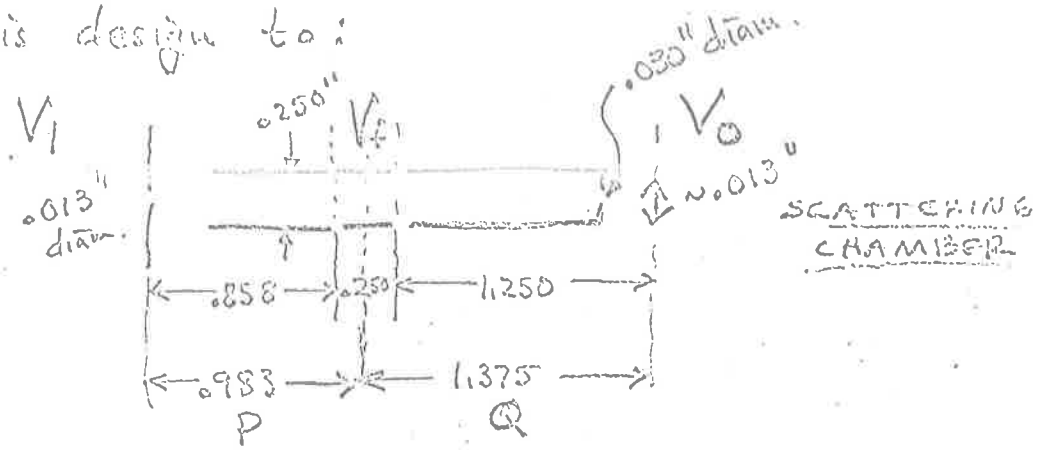

The next step was to find out if this lens actually performed as desired. For $V_1 = 25$ and 70 eV, and $V_o = 20$ to 400 eV, the matrix method of calculation was used to find the focusing voltage by trial and error. One of these calculations was reproduced in lecture 2.

Curves for V_f versus V_o, with $V_1 = 70$ and 25 eV were obtained and are shown in the attached figure. It was found that focusing could be obtained with either a low or a high voltage. We prefer the high-voltage mode for actual operation.

Voltage operating points found empirically were in rough agreement with those calculated, if the beam was focused into a Faraday cup in the scattering chamber. When adjusting the beam for

maximum transmission through the scattering chamber the operating voltages were somewhat different.

The lens matrices were used to calculate the electron beam profile in the scattering chamber. The center and extreme rays of the center and extreme pencils were calculated. (as in the example in lecture 2) Some of these rays are shown in the attached figure. In all cases the exit pupil was to the left of the scattering chamber, so that the beam diverged after the image. If the exit pupil could have somehow been shifted to the right of the diagram, then the beam would have converged after the image, although at the expense of being larger at the entrance aperture to the scattering chamber.

Manipulation of the exit pupil will be discussed in a later lecture.

We have now finished the design of a variable ratio lens, capable of producing useful beams over a wide range of final energies. It could be attached to an electron monochrometer to produce a variable-energy monoenergetic beam, or to an electron gun to produce a variable energy beam.

Combination of Two Simple Lenses

As a final example of simple lens systems, consider a lens made up of two simple lenses. For example, using tube lenses:

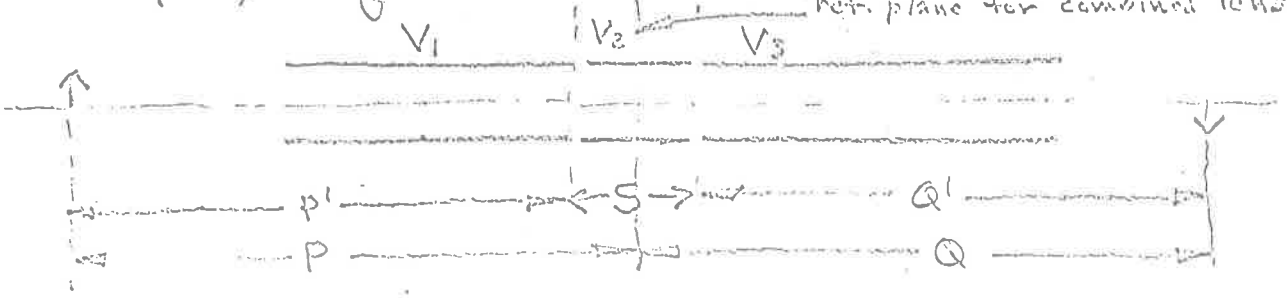

$$p' = p - \frac{\xi}{2} \qquad Q' = Q - \frac{\xi}{2}$$

The overall properties of this compound lens could be found by graphical ray construction, by algebraic equations, or by use of the matrix method.

We will use the matrix method because it is the easiest to apply.

Matrix for first lens: $[f_1, f_2, F_1, F_2]$

$$\mathcal{M}_1 = -\frac{1}{f_2}\begin{pmatrix} S - F_2 & (p' - F_1)(S - F_2) - f_1 f_2 \\ 1 & p' - F_1 \end{pmatrix}$$

Matrix for second lens: $[f_1', f_2', F_1', F_2']$

$$\mathcal{M}_2 = -\frac{1}{f_2'}\begin{pmatrix} Q' - F_2' & -F_1'(Q' - F_2') - f_1' f_2' \\ 1 & -F_1' \end{pmatrix}$$

$$\mathcal{M}_2\mathcal{M}_1 = \frac{1}{f_2 f_2'}\begin{pmatrix} (Q' - F_2')(S - F_2) - F_1'(Q' - F_2') - f_1' f_2' & \cdots \\ (S - F_2) - F_1' & (p' - F_1)(S - F_2) - f_1 f_2 - F_1'(p' - F_1) \end{pmatrix}$$

$$= \frac{1}{f_2 f_2'}\begin{pmatrix} Q'(S - F_1' - F_2) - F_2'(S - F_1' - F_2) - f_1' f_2' & \cdots \\ S - F_1' - F_2 & p'(S - F_1' - F_2) - F_1(S - F_1' - F_2) - f_1 f_2 \end{pmatrix}$$

$$= \frac{S - F_1' - F_2}{f_2 f_2'} \begin{pmatrix} q' - F_2' - \dfrac{f_1' f_2'}{S - F_1' - F_2} & -1 \\ 1 & p' - F_1 - \dfrac{f_1 f_2}{S - F_1' - F_2} \end{pmatrix}$$

Hence, by comparing with form for a single lens,

$$\begin{cases} f_2^* = \dfrac{f_2 f_2'}{F_1' + F_2 - S} & \text{by symmetry, } f_1^* = \dfrac{f_1 f_1'}{F_1' + F_2 - S} \\ F_1^* = F_1 - \dfrac{f_1 f_2}{F_1' + F_2 - S} + \dfrac{S}{2} & F_2^* = F_2' - \dfrac{f_1' f_2'}{F_1' + F_2 - S} + \dfrac{S}{2} \end{cases}$$

If desired, these equations can be used to obtain the focal points and focal lengths of a combination of two or more single lenses.

Einzel Lens

A particularly useful special case of the above is the Einzel lens:

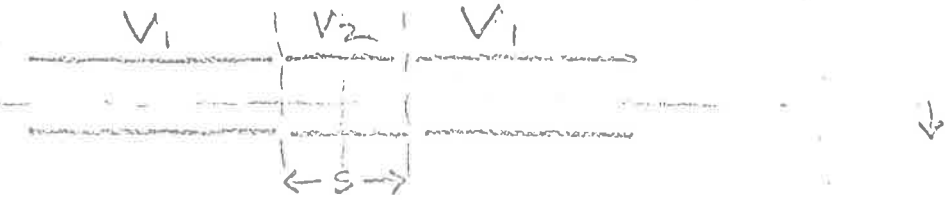

The two identical lenses must be placed sufficiently far apart so that the fields of the two simple lenses have small overlap. A two-diameter spacing would probably be sufficient. For an especially compact lens, one might use a one-diameter spacing, but the resultant f, F's would only be approximated by the calculated values.

In the equation for the general pair of lenses, we make the substitutions:

$$\begin{cases} f_1' \longrightarrow f_2 \\ f_2' \longrightarrow f_1 \\ F_1' \longrightarrow F_2 \\ F_2' \longrightarrow F_1 \end{cases}$$

There results:

$$\begin{cases} f_1^* = f_2^* = \dfrac{f_1 f_2}{2F_2 - S} \\ F_1^* = F_2^* = F_1 - f_1^* + \dfrac{S}{2} \end{cases}$$

Such an Einzel lens has been used as a Field Lens in the Model B scattering apparatus, and will be described later.

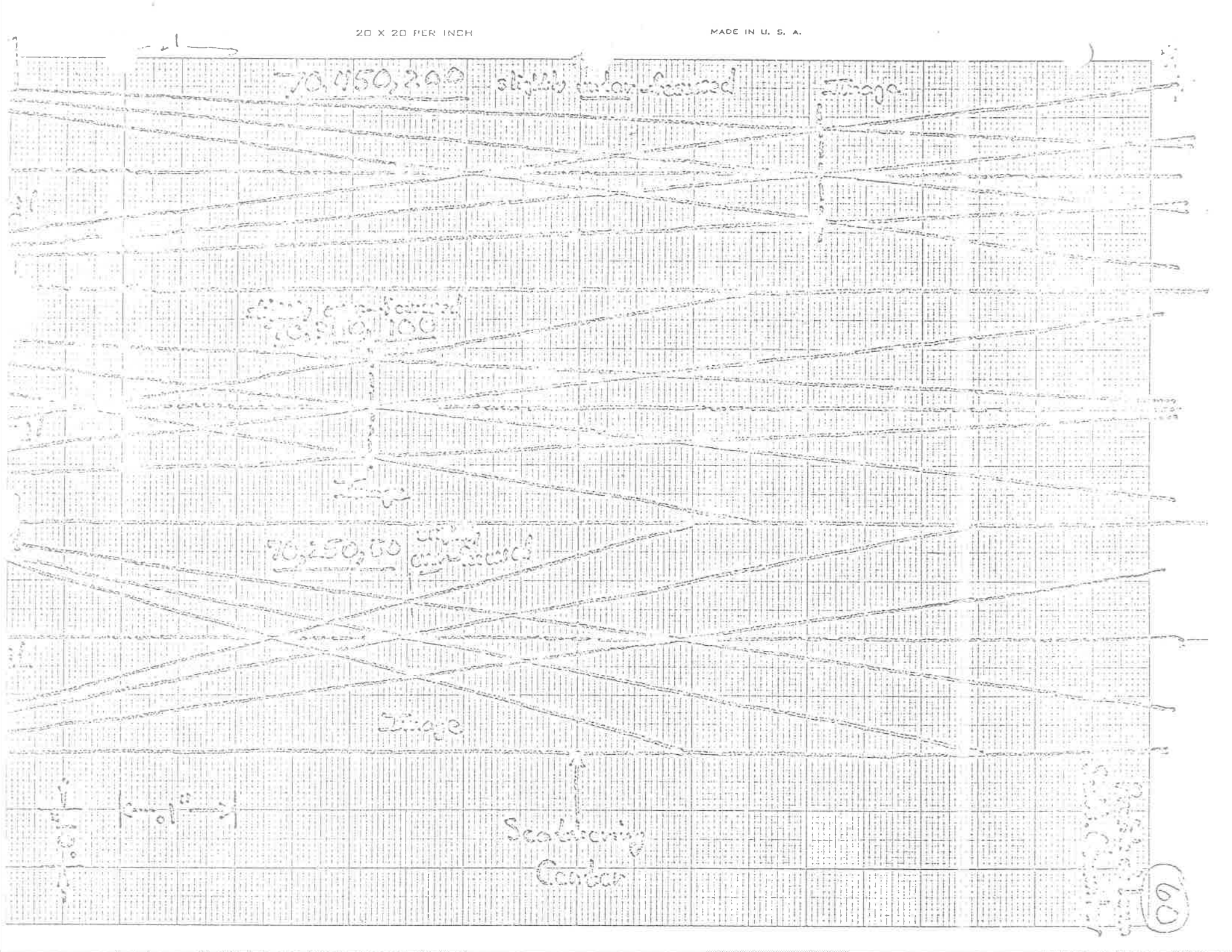

Electron optics lecture ①

Lecture 4

May 13, 1987

A.P. Banford, "The Transport of Charged Particle Beams", E. & F.N. Spon Limited, London (1966)

This book uses the matrix technique for the design of charged particle optics. The application of Liouville's theorem is explained, and its relation to R-θ diagrams is presented. R-θ diagrams are consistently used. All of the examples relate to the transport of high energy beams from accelerators, but the methods are equally useable for low energy beams. The treatment is self-contained and very readable.

Windows and Pupils

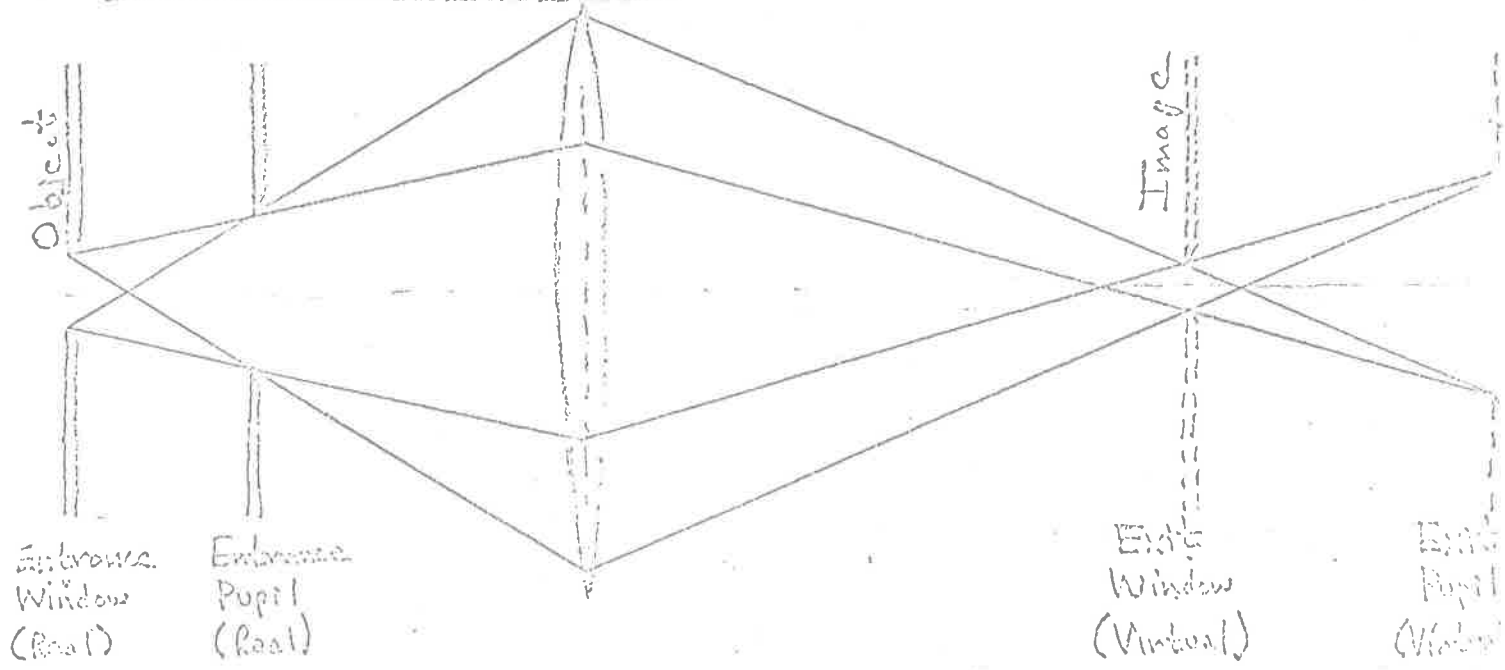

In the diagram the object size is defined by a real aperture called the entrance window. The angular extent of rays accepted by the system from each object point is defined by means of a real aperture called the entrance pupil. In a well-designed optical system no other apertures or lens edges would limit the rays accepted by the system. If the rays are so limited, then the angular range of rays accepted will depend on position in the object plane, and the intensity in the image plane will depend on position. Such a system is said to suffer from vignetting and is a condition to be avoided.

The image of the entrance window is called the exit window, and the image of the entrance pupil is called the exit pupil. The angular extent of rays in the image plane is exactly the same as if the virtual exit window and pupil were replaced by real apertures and the real entrance window and pupil were removed.

Other combinations are also possible, for example, a real entrance window and a real exit pupil. However, this arrangement is not recommended for electron optical systems with variable lenses, because one is likely

to adjust the lens for maximum electron transmission, which would probably result in placing the exit window and pupil in coincidence and destroying the desired angular collimation.

Also, the technique of using a lens edge as a pupil, common in light optics, is not recommended for electron optical systems, since aberrations become very large when electrons are near the lens edge.

It is therefore recommended that a real window and pupil be placed in the object space, in the intermediate image space, or in the final image space. Usually it is desirable to place the real window and pupil as early in the system as possible, so that unwanted electrons have the least chance to cause trouble.

In a more complicated system, containing several lenses and apertures, there may be some doubt as to the identity of the window and pupils. For this case one should construct images of all the limiting elements in one space, say the final image space. It will then be clear which are the limiting elements. If there are more than two limiting elements there is vignetting and the placement of apertures should be modified.

Necessity for Control of Pupil

In most electron optical systems it is necessary to control not only the exit window (final image) but to control the exit pupil, since the exit pupil controls the angular relations in the final electron beam.

Note that the Helmholz–Lagrange law will determine the angular extent of the pencil of rays forming each image point, but that the angle of the pencil with respect to the axis depends on the pupil position and size.

Example of Bad Pupil Location

Many electron optical systems suffer from bad pupil location. A particularly bad arrangement occurred in one of our own designs.

The next diagram shows a thin-lens analog of the situation we encountered. Object A is imaged at A' by lens B, and this image is further imaged at A'' by lens C, as indicated by the solid rays. Note the very large angle of the pencils with respect to the axis. The exit pupil, at the point where the central ray crosses the axis, is very small

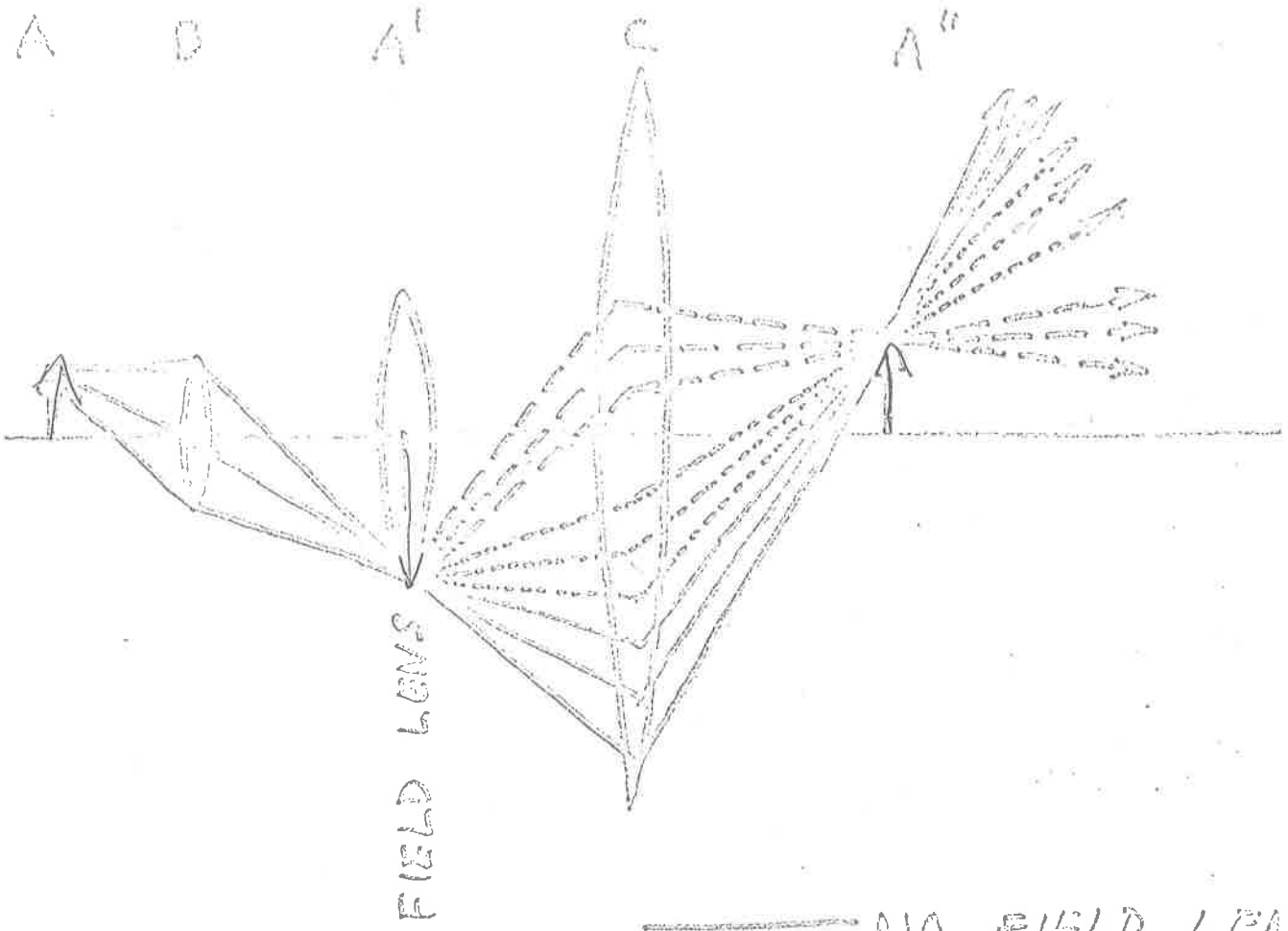
A
B
A'
C
A''
FIELD LENS
NO FIELD LENS
WITH FIELD LENS

The next diagram is a schematic of the actual electron optical system. Vertical dimensions are stretched a factor of four with respect to horizontal dimensions. Solid lines show the calculated rays without the field lens. Notice that a large fraction of the electrons are lost at the last lens. [The discontinuity in rays across the lenses is a result of extrapolating the distant rays into the center of the lens. The rays are actually connected by smooth curves.]

With the field lens at optimum strength the central ray of the final pencil is parallel to the axis, as required, and no electrons are lost at the final lens.

Energy Add lens

Another application of the field lens is to the problem of the energy analyzer. In order to maintain the electron optics of the analyzer fixed over an energy loss scan, and thereby keep the same energy resolution, it is necessary to add back the energy which was lost. This energy must be added back in a way which disturbs the electron optics

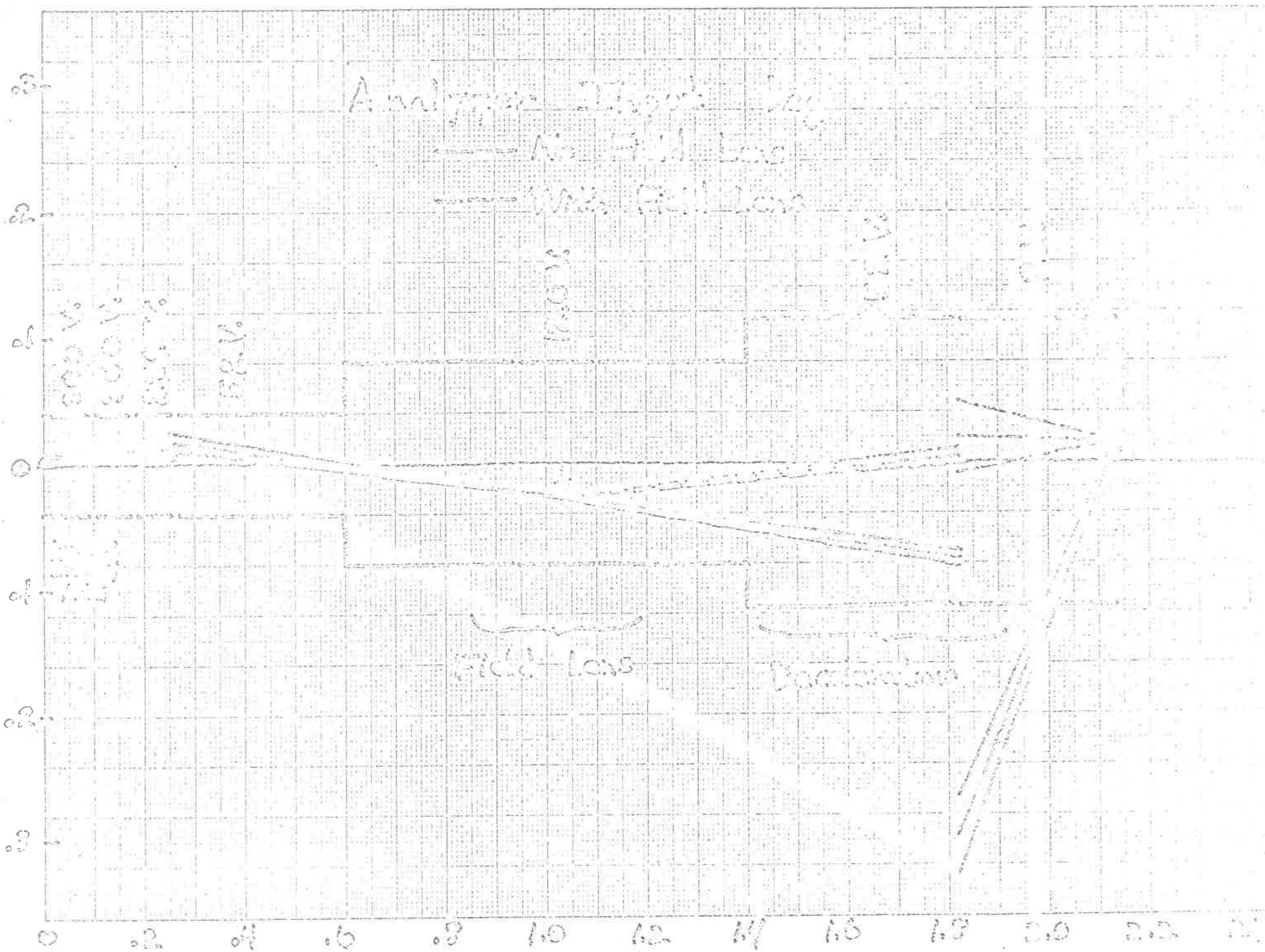
No Field Loss
With Field Loss
Field Loss
0
1.0
1.2
1.6
1.8
2.0

of the analyzer as little as possible.

A solution which works well in practice is the following:

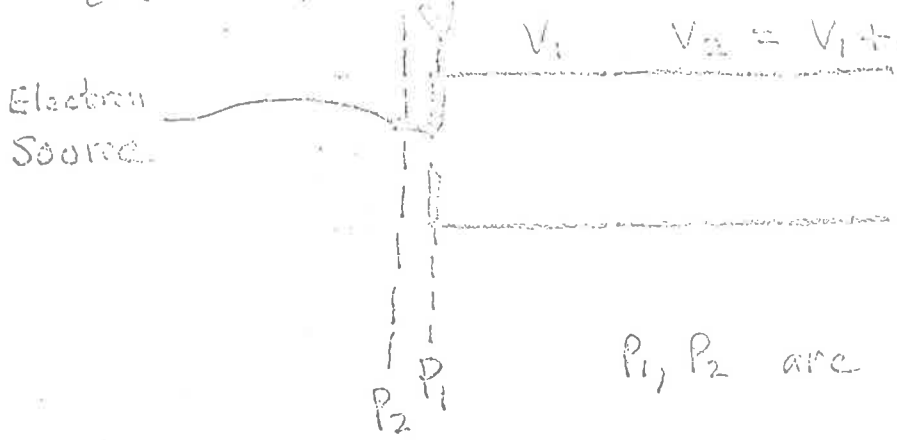

P_1, P_2 are principle planes.

From the properties of thick lenses, an electron source at the first principle plane is imaged with unity magnification onto the second principle plane. For a strong lens, $V_2/V_1 \geq 3$, the position of the principle planes is nearly constant and their separation is small. We can therefore add energy to the electron beam and change the effective source location very little. The pencil angles must, of course, change so as to satisfy the Helmholtz-Lagrange law. In practice the energy add lens works well for $V_2/V_1 < 3$, because as the lens becomes weak and does little to the electrons.

We have used this energy add lens in our angular scattering apparatus. We also used it in the design of a photodetachment energy analyzer for

found for a range of initial conditions. A group of computer programs was therefore written to perform these lens calculations automatically.

At the present time these programs can only deal with tube lenses, and their accuracy is limited by the accuracy of Spangenberg's data, which is perhaps 20% for individual lens parameters. Nevertheless, the program gives a good indication of the qualitative performance of a lens system, and in some cases gives good quantitative results.

Each program is in the form of a subroutine:

1) LENS.

Given the size, position, and voltages for a system of tube lenses, the program calculates the Gaussian electron rays entering and leaving each lens. Detailed trajectories inside the lens fields are not calculated. A window and pupil at the beginning of the system are used to specify the incident rays, and the position and size of the window and the pupil as well as the beam and pencil angle are determined after each lens. The print-out

can include the focal properties of each lens, the matrix for each lens, and the after each lens. A sample print-out is shown on the next page.

2) IMAGE

Adjusts a specified voltage to find the voltage or voltages which give an image in a specified position.

3) FIELD

Adjusts the voltage on a field lens until a specified beam angle is obtained.

H) INTER

A somewhat specialized program which checks a particular lens for the formation of a real intermediate image.

⇒ All programs use a standard block of DIMENSION, COMMON, and REAL statements.

The options on these subroutines are as follows:

CALL LENS (JJ, KK, LL, MM) Reads in data

CALL LENSI (JJ, KK, LL, MM) Does not read in data

JJ=0 DON'T } Print out lens data, windows, pupils
JJ≠0 DO } and end points of electron rays.

KK=0 DON'T } Print out electron trajectories at
KK≠0 DO } 100 equally spaced points.

LL=0 DØN'T } Plot and printout electron trajectories at
LL≠0 DØ } 100 equally spaced points.
Not yet working on UNIVAC 1108.

MM — does nothing

CALL LENS2 (---, ---, ---, etc) — All input data are included in the subroutine call. None are read in.

CALL IMAGE (L, M, N, POSIMG, TOL, V1, V2, DELV, NIMG, POTIMG, JJ)

L=1	find image at voltage nearest to V1
L≠1	find all images in voltage range V_1 to V_2.
M	index of voltage to be adjusted
N	index of image to be found
PØSIMG	desired position of image
TØL	tolerance on image location
DELV	tolerance on image voltage
NIMG	number of images found
PØTIMG	imaging potentials (max. of 5)

· Note — Always check for NIMG=0 before proceeding.

CALL FIELD (M, N, DELV, BA, TOL, JJ)

M	index of imaging potential to be used in print
N	index of field lens potential
DELV	tolerance on voltage adjustment
BA	desired beam angle
TOL	tolerance on beam angle
JJ=0	Don't } Print out complete
JJ≠0	Do } lens data at adjustment.

One line is printed for each voltage tried.

CALL INTER (NIMG, M, L, BEGIN, END, XINTER, POTIMG)

NIMG	number of possible intermediate images
M	index of lens which forms intermediate image.
L	number of actual intermediate images.
BEGIN	beginning of allowed range of positions
END	end of allowed range of positions
XINTER	position of intermediate image
POTIMG	voltage which gives the intermediate image.

Program examples will be given in the next lecture.

Lecture 5 May 23, 1967

Design of High-Current Low-Voltage Electron Guns

Before we can design a high-current low-voltage electron gun, it is necessary to consider the limits which space charge places on the maximum current in an electron beam.

Space-Charge Limited Current

Assume that the region through which the maximum amount of current is to be sent is a tube of diameter D and length L:

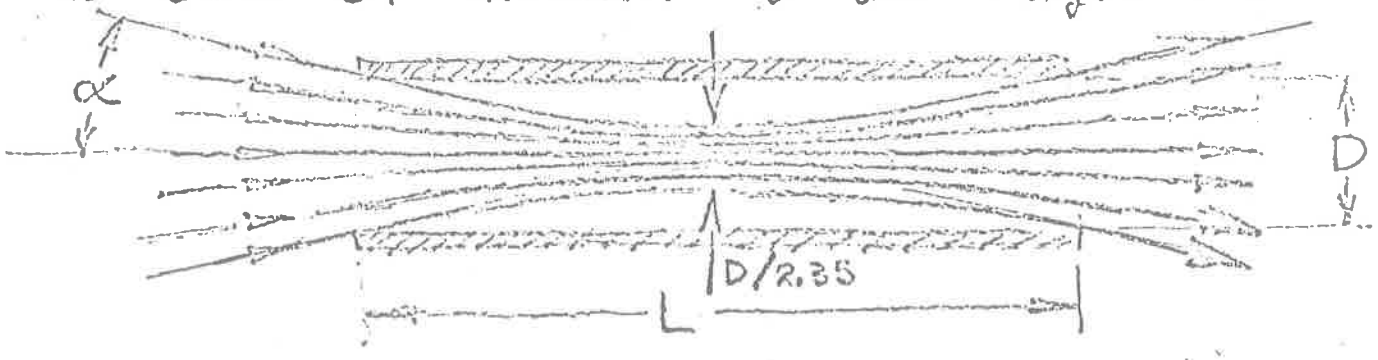

From the standard treatments of the space-charge problem (Pierce or Spangenberg, e.g.), the maximum current through the tube is achieved by directing the electron beam at the center of the tube. The maximum current is given by

$$I = 38.5\, V^{3/2} \left(\frac{D}{L}\right)^2 \qquad I: \mu\text{amp} \qquad V: \text{volts} \qquad (1)$$

In terms of the angle α,

$$I = 38.5 V^{3/2} \alpha^2 \qquad (2)$$

[Note: The constant k in $I = kV^{3/2}$ is often called the <u>microperveance</u>]

As an example, suppose $V = 1$ Volt, $\alpha = 0.1$ rad. Then $I = 0.0385$ amp.

If <u>more</u> than the maximum current is injected into the tube, the space charge spreading will increase, with the result that <u>less</u> current will emerge from the tube. The books by Pierce and Spangenberg give design curves which allow the profile of any beam to be calculated. Glaser's book gives similar information for an initial beam which is not directed at a point.

The minimum diameter of the beam is $D/2.35$.

Note that space charge places a limit on total current and <u>not</u> on current density, since only the <u>ratio</u> of D and L is involved. Any current density is possible by reducing D and L, if a suitable source is available.

Multi-Stage Guns

Simpson and Kuyatt, J. Research NBS, 67C, 279 (1963), have shown that, to produce the maximum space-charge limited current at low voltages, it is necessary to form a beam at a higher voltage and then decelerate to the desired low voltage. Two guns of this type are described in R.S.I. 34, 265 (1963). Another more versatile gun will be described in this lecture. This gun is used in our high-current monochromator. [R.S.I. 38, 103 (1967)].

Diode Stage

In order to form a beam of known current density and geometry, we decided not to use the usual triode gun, but to start with the space-charge limited diode as our initial electron source.

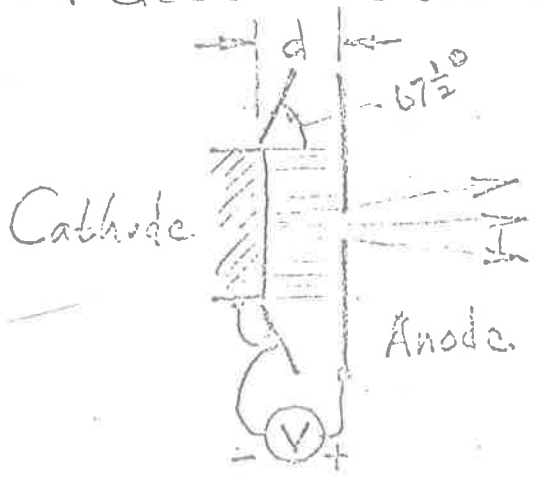

$$J = 2.33 \frac{V^{3/2}}{d^2} \qquad (3)$$

If d in cm., J is in $\mu A/cm^2$.

If d in inches, J is in $\mu A/in^2$, etc.

We see right away that the space-charge limited current density J is easily calculated from the voltage and the spacing of the diode.

The angular characteristics of the beam emerging from the anode hole must also be known.

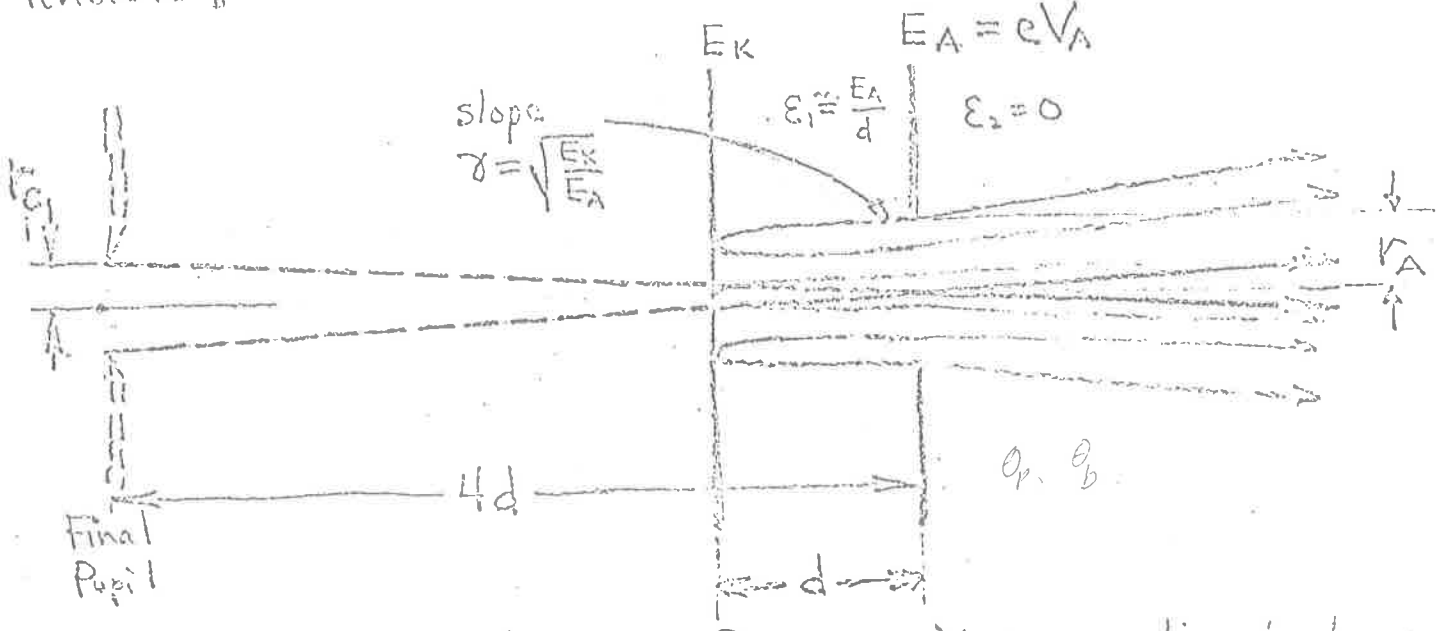

Let $E_K = kT$. By considering only electrons of energy E_K emitted from the cathode a good approximation to the beam properties can be obtained. Further assume that the anode hole can be treated as a thin lens (Calbick lens) of focal length $\frac{4V_A}{\mathcal{E}_2 - \mathcal{E}_1} = \frac{4V_A}{-\frac{V_A}{d}} = -4d$.

Assumes uniform field

An electron emitted parallel to the cathode has slope $\gamma = \sqrt{\frac{E_K}{E_A}} = \sqrt{\frac{V_K}{V_A}}$ when it reaches the anode hole. (From energy considerations alone.)

Take the anode hole to be the window for the system. This window, before the Calbick lens, is formed by pencils with half angle γ, and with the central ray parallel to the axis. Hence the pupil, before the Calbick lens, is at infinity.

After the Calbick lens, the pupil is $4d$ to the left of the anode. Its size can be found by extrapolating back a ray of slope γ from the center of the Calbick lens.

$$r_c = 4d\gamma \tag{4}$$

Since the initial and final windows are identical the magnification is one, and the pencil half-angle remains unchanged and equal to γ. The beam half-angle depends on the size of the anode hole:

$$\Theta_b = \frac{r_A}{4d} \tag{5}$$

Combining equations, the Richardson-Dushman divided by voltage is given by:

$$\frac{R}{V_A} = \frac{J}{\Omega V_A} = \frac{2.33 \frac{V_A^{3/2}}{d^2}}{\pi \gamma^2 V_A} = .074 \frac{V_A^{3/2}}{V_K d^2} \qquad (6)$$

$$\left[V_K = \frac{T_K(^\circ K)}{11,600} \right]$$

Finally, the total current from the diode is

$$I_{total} = JA = 2.33 \frac{V_A^{3/2}}{d^2} \pi r_A^2 \qquad (7)$$

$$= 7.32 V_A^{3/2} \frac{r_A^2}{d^2}$$

In an actual diode electrons are emitted from the cathode with a Maxwellian distribution of energies. The radius of the pupil, and therefore the beam angle, depend on the energy of emission and hence are not sharp. Glaser, for example, shows that the final pupil has a Gaussian distribution of intensity with a FWHM of $2r_c$, and our approximation is quite reasonable.

Note that the Richtstrahlwert does not depend on the detailed electric field in the diode, even though the pupil size, pupil location, and beam angle do depend on the electric field at the cathode.

The above assumed uniform field in the diode. In a space-charge limited diode, the electric field is:

$$\mathcal{E}(x) = \frac{4 V_A}{3 d^{4/3}} x^{1/3} \qquad (8)$$

The focal length of the Calbick lens is then $-3d$, the final pupil is $3d$ to the left of the anode hole, and the beam angle is

$$\theta_b = \frac{r_A}{3d} \qquad (9)$$

The Richtsteinwert and pencil angle remain unchanged.

Design of Gun with Diode

Assume that the final beam is space-charge limited, voltage V, convergence half-angle α, and non-space-charge radius r. (In practice, r can be made close to the minimum radius of the space charge beam.) For this beam

$$\frac{R}{V} = \frac{I/\pi r^2 \pi\alpha^2}{V} = \frac{38.5 V^{3/2} \alpha^2}{V \pi r^2 \pi \alpha^2} = 3.9 \frac{V^{1/2}}{r^2} \qquad (10)$$

The diode parameters should be chosen to give this value of R/V.

Example $V = 1$ Volt $r = .1$ mm

$$\frac{R}{V} = 390$$

Suppose $d = 4$ mm, $V_K = 0.1$ Volt (Oxide Cathode)

Then

$$390 = .74 \frac{V_A^{3/2}}{.1 \times 16}$$

$$V_A^{3/2} = \frac{390 \times 16}{7.4} = 844$$

$$V_A \cong 92 \text{ Volts}$$

The current density at the diode:

$$J = 2.33 \frac{V_A^{3/2}}{d^2} = 2.33 \frac{(844)}{(.4\text{cm})^2} = 12{,}300 \frac{\mu A}{cm^2}$$

To get a well-collimated final beam, use a fixed-ratio decelerator as the final element, with aperturing on the high-voltage side. Since the diode voltage and the input voltage to the decelerator are fixed by these considerations, we need an energy changing lens. This lens should be capable of operation over a wide range, so current can be varied with diode voltage; and final energy can be adjustable. Suppose this is a three-tube lens?

System now is:

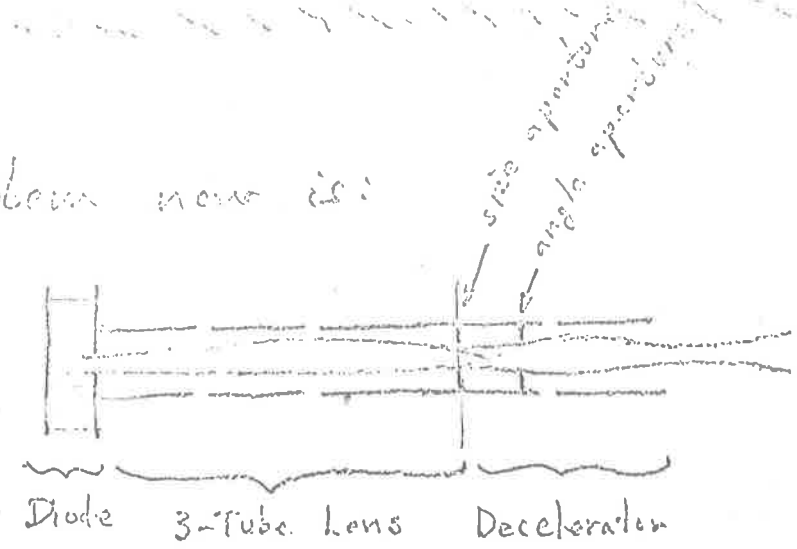

Conditions on Decelerator

The final beam should be space-charge-limited. Before deceleration we would like space charge effects to be negligible so that the defining apertures will accurately collimate the electron beam, and so that current will not be lost due to space-charge spreading.

Input conditions: V_1, α_1

Output conditions: V_2, α_2, M

Final current: $I = 38.5\, V_2^{3/2} \alpha_2^2$

Helmholtz-Lagrange: $\sqrt{V_1}\,\alpha_1 = M\sqrt{V_2}\,\alpha_2$

Space Charge Limit to Input Current: $38.5\, V_1^{3/2} \alpha_1^2$

$$\frac{\text{Input Current}}{\text{Max. possible Input Current}} = \frac{V_2^{3/2}\alpha_2^2}{V_1^{3/2}\alpha_1^2} = \frac{V_2^{3/2}}{V_1^{3/2}}\,\frac{V_1}{M^2 V_2} = \frac{V_2^{-1/2}}{V_1^{1/2} M^2}$$

Use H-L to eliminate α_2/α_1:

Example Let $\frac{V_1}{V_2} = 10$. For 0.1 of space-charge-limited current at input,

$$\frac{.1}{M^2} = .1 \Rightarrow \underline{M = 1}$$

In our actual design of such a gun, we used $M = 1.5$, $\frac{V_1}{V_2} = 10$, giving as the fraction of the space-charge-limited current

$$\frac{.1}{(1.5)^2} \cong .045.$$

The design of the decelerator was given in Lecture 3.

$$\begin{cases} \frac{V_1}{V_2} = 10 & \alpha_2 = .071 \text{ rad.} \quad M = 1.5 \\ & \alpha_1 = .0336 \text{ rad} \\ & \text{Final diam.} = .020". \end{cases}$$

Diode Parameters — spacing .215"

Case 1 $V_1 = 2.5$ Volts

Use Eqs. (6) and (10) to get diode voltage

$$.074 \frac{V_A^{3/2}}{.1(.215)^{3/2}} = 3.9 \frac{(2.5)^{3/2}}{(.01)^{3/2}} \Rightarrow V_A = 39.7 \text{ Volts}$$

Oxide Cathode $V_K \cong .1$ Volts

$$J = 2.33 \frac{V_A}{d^2} = 2.33 \frac{(39.7)}{(.215)^2} = 1940 \frac{mA}{in^2} \cong 300 \mu A/cm^2$$

Case 2

$V_1 = 7$ Volts

$\Rightarrow V_A = 74.5$ Volts

$$J = 2.33 \frac{(74.5)^{3/2}}{(6.25)^2} = 32{,}500 \frac{\mu A}{in^2} = 5040 \frac{\mu A}{cm^2}$$

The cathode current densities are low, as is usually the case for low-voltage guns.

Note: Combining eqs (3), 6), (7) gives

$$J = 12.3 \frac{V_1^{3/2} V_K}{p^2}$$

For oxide cathode: $V_1^{3/2}$

$$J = 1.23 \frac{\quad}{p^2}$$

R-θ Diagrams

Before continuing with the gun design started in the last lecture, I will give some further information on the R-θ diagrams, which were briefly introduced in Lecture 1.

Consider a beam formed by two real or virtual apertures:

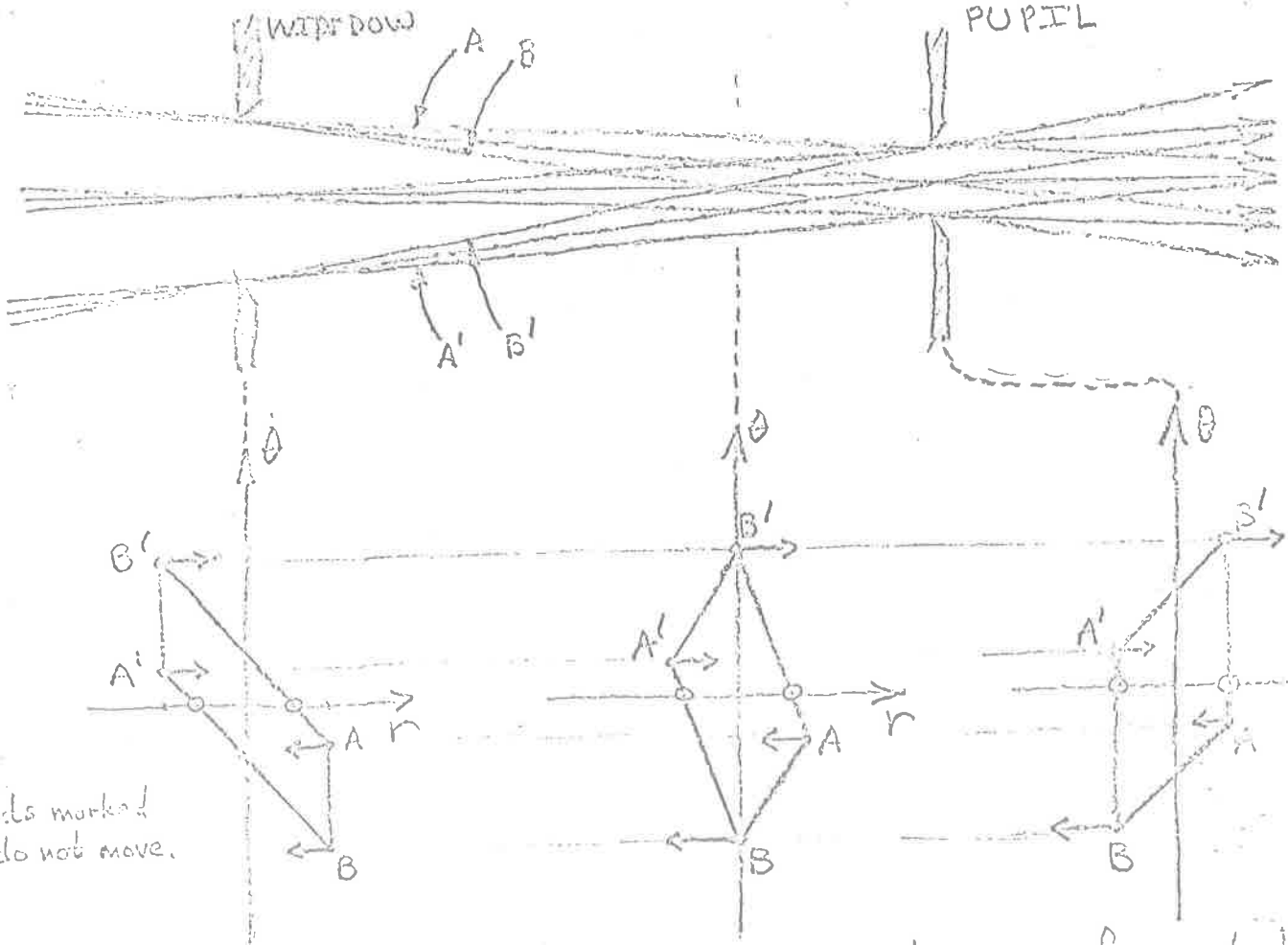

Note that the corners are always formed by the rays A, A', B, B'. As we move along the beam, the positive angle corners move to the right, and the negative angle corners move to the left on the diagram.

R-θ Diagrams

Given: Window, Pupil, Position z from Windows.
Construct: R-θ Diagram at z.

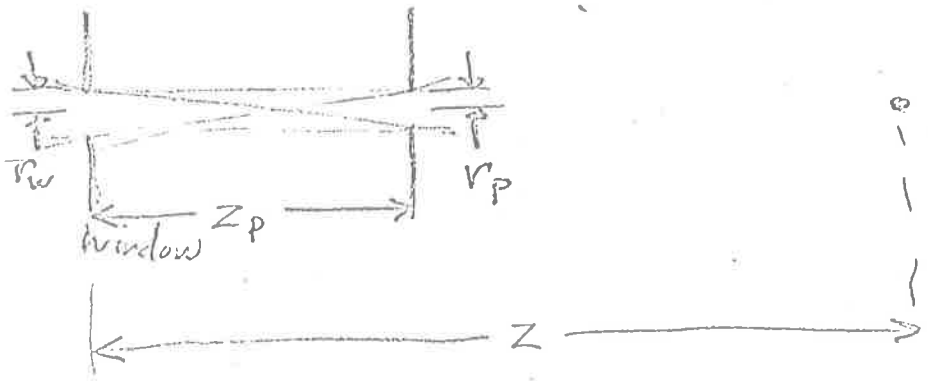

At window, corners of R-θ diagram are:
assuming r_w, r_p are positive.

$$\left\{ \begin{array}{l} \left(r_w, \frac{r_p - r_w}{z_p} \right) \\ \left(r_w, \frac{r_p + r_w}{z_p} \right) \\ \left(-r_w, \frac{-r_p + r_w}{z_p} \right) \\ \left(-r_w, \frac{-r_p + r_w}{z_p} \right) \end{array} \right.$$

At position z:
(Corners move in r a distance zθ)

$$\left\{ \begin{array}{l} \left(r_w + \frac{z}{z_p}(r_p - r_w), \frac{r_p - r_w}{z_p} \right) \\ \left(r_w + \frac{z}{z_p}(+r_p - r_w), \frac{-r_p - r_w}{z_p} \right) \\ \left(-r_w + \frac{z}{z_p}(-r_p + r_w), \frac{-r_p + r_w}{z_p} \right) \\ \left(-r_w + \frac{z}{z_p}(-r_p + r_w), \frac{r_p + r_w}{z_p} \right) \end{array} \right.$$

Beam Angle : $r_w / z_p = \theta_b$

Pencil Angle : $r_p / z_p = \theta_p$

r_w, r_p: positive

z_p: positive if pupil to right of window

At window, corners of R-θ diagram are:

$(r_w, \theta_p - \theta_b)$
$(r_w, -\theta_p - \theta_b)$
$(-r_w, -\theta_p + \theta_b)$
$(-r_w, \theta_p + \theta_b)$

At position z, corners of R-θ diagram are:

z measured from window

$(r_w + z(\theta_p - \theta_b), \theta_p - \theta_b)$
$(r_w + z(-\theta_p - \theta_b), -\theta_p - \theta_b)$
$(-r_w + z(-\theta_p + \theta_b), -\theta_p + \theta_b)$
$(-r_w + z(\theta_p + \theta_b), \theta_p + \theta_b)$

At pupil, corners of R-θ diagram are:

$(r_p, \theta_p - \theta_b)$
$(-r_p, -\theta_p - \theta_b)$
$(-r_p, -\theta_p + \theta_b)$
$(r_p, \theta_p + \theta_b)$

Assume that we have an electron optical device in which the final window is fixed in size and position, but the position of the pupil is variable. As the position of the pupil changes, the pupil size changes also, but the Helmholtz-Lagrange law assures us that the pencil angle, θ_p, must be a constant. It follows that the pupil size must be proportional to its distance from the window: $r_p = z_p \theta_p$. The distance of the pupil from the window also determines the beam angle: $\theta_b = r_w / z_p$.

The next figure is an R-θ diagram at a fixed window with increasing beam angle. Decreasing beam angle would give R-θ diagrams reflected about the θ axis.

Electron Gun Design

The electron gun design started in Lecture 5 will now be completed.

Design so far is:

Constant Gap

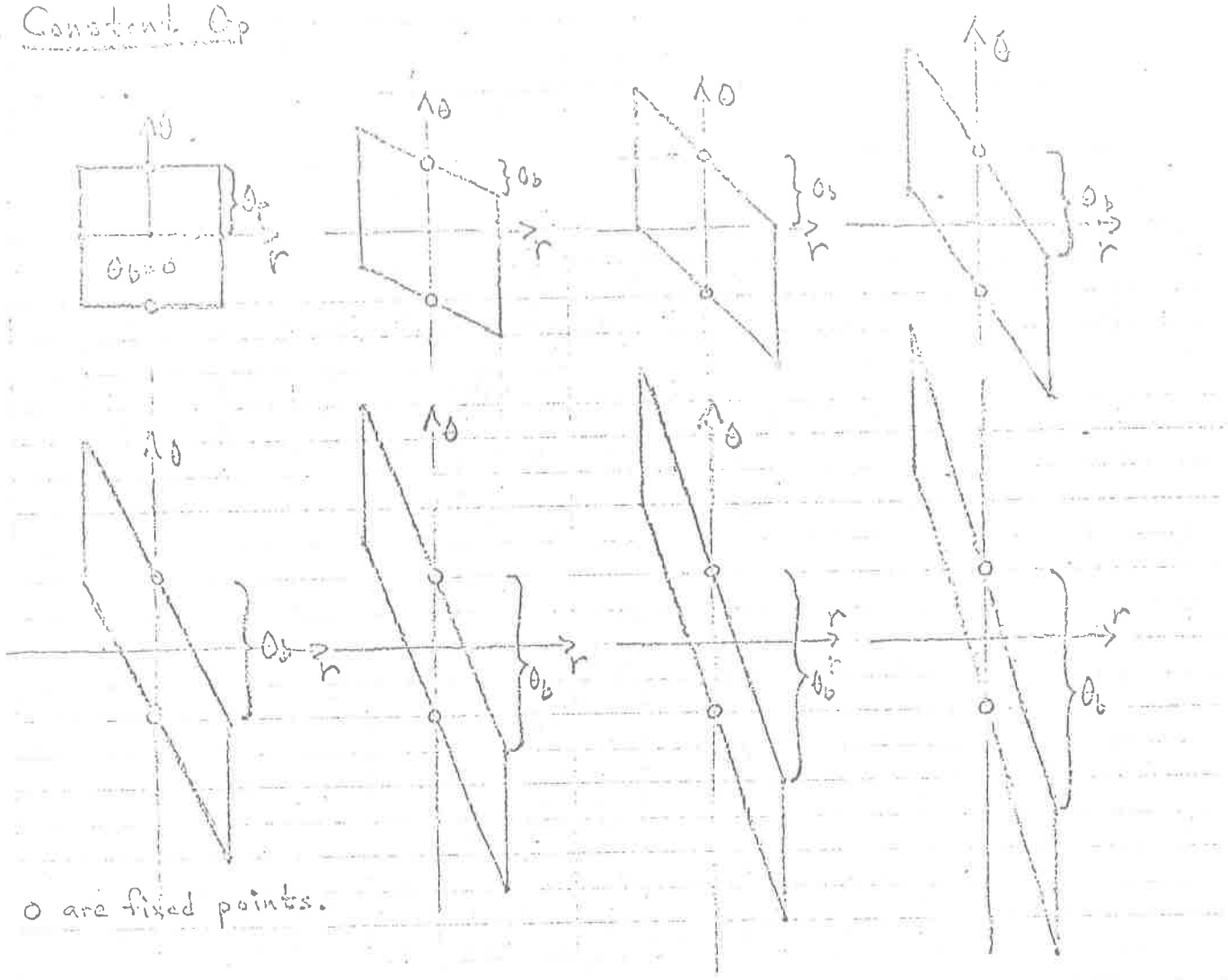

o are fixed points.

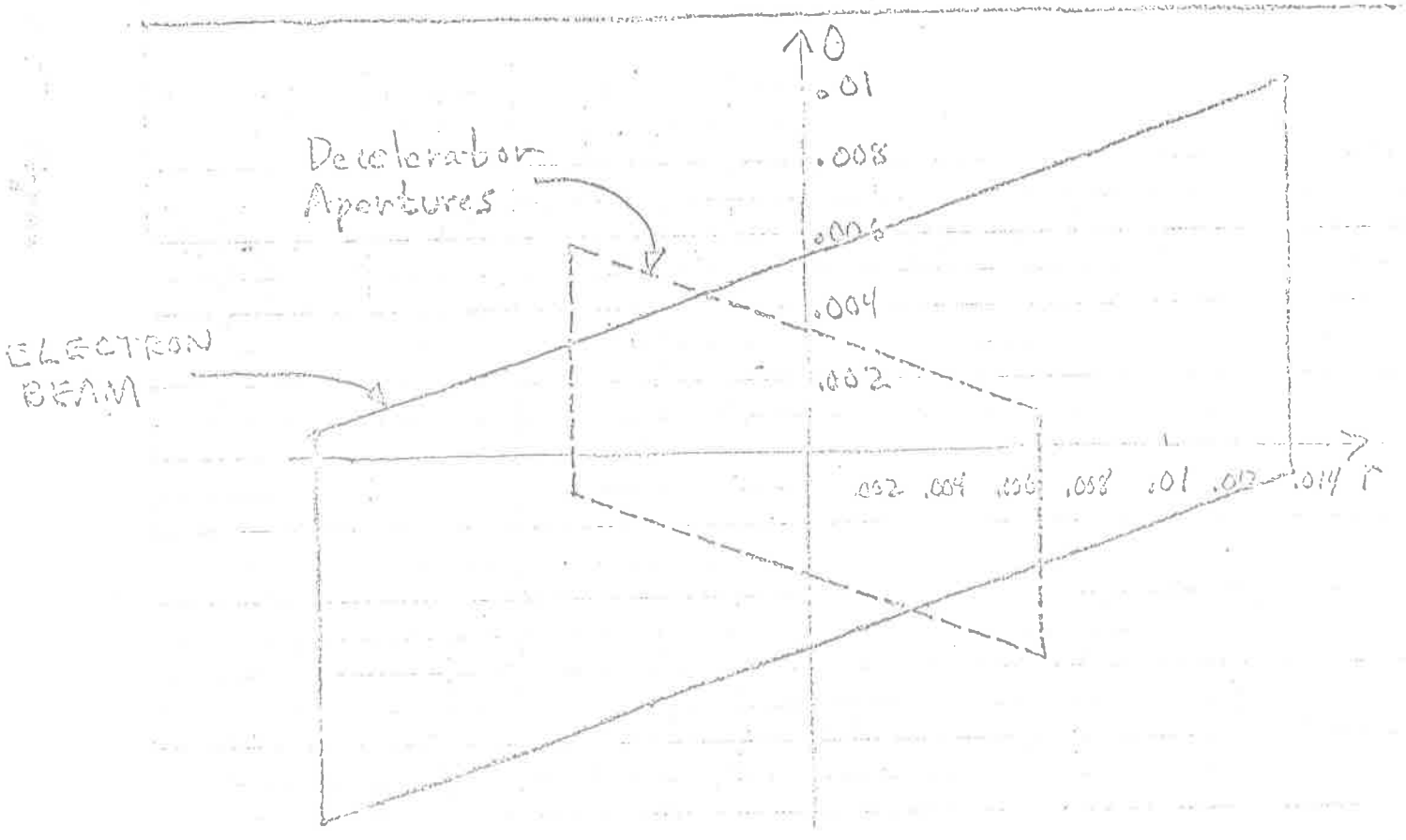

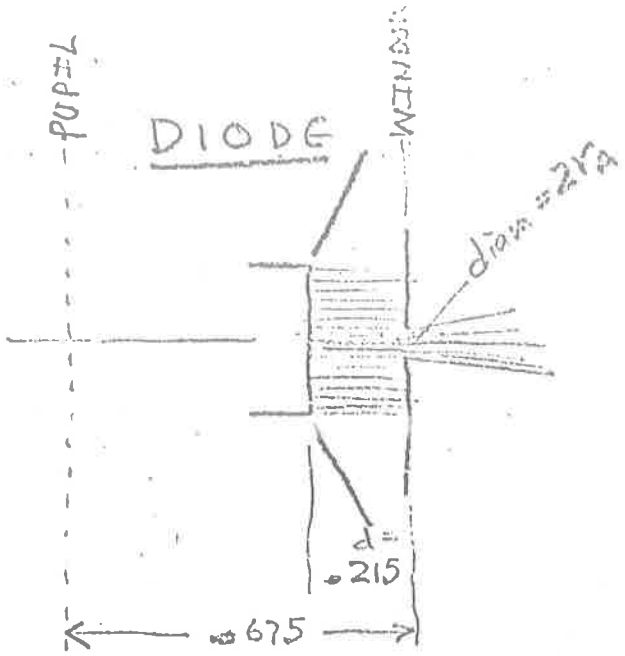

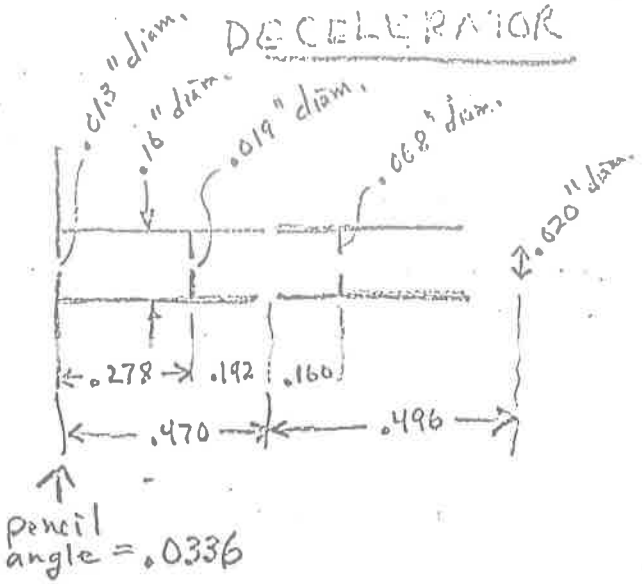

Case 1	0V.	75V.	70V.	7V.
Case 2	0V.	40V.	25V.	2.5V.
		E_a	E_o	

Let's start out by assuming that the anode hole of the diode is imaged onto the .013" diam. entrance aperture of the decelerator with constant magnification. In order to make line-up uncritical, make anode hole about twice as big as necessary, say, .024" diam. In this way, edge effects of the anode hole lens will also be avoided.

Minimum magnification between diode and decelerator is reached when image of anode hole is reduced to .013" diam.: $M_{min} = \frac{.013}{.024} = .54$.

Maximum magnification is reached when the final pencil angle is reduced to .0336 rad.

Pencil angle at diode	Beam angle at diode
Case 1 $\theta_p = \sqrt{0.1/75} = .0365$ rad.	$\theta_b = r_a/3d = \frac{.012}{.675}$
Case 2 $\theta_p = \sqrt{0.1/40} = .05$ rad.	$= .0178$ rad.

Case 1 $\sqrt{75}\,(.0365) = M_{max}\sqrt{70}\,(.0336)$

$$M_{max} = \sqrt{\frac{75}{70}}\,\frac{.0365}{.0336} = 1.13$$

Case 2

$\sqrt{40}\,(.05) = M_{max}\sqrt{25}\,(.0336)$

$$M_{max} = \sqrt{\frac{40}{25}}\,\frac{.05}{.0336} = 1.88$$

Since $\theta_p = \sqrt{\frac{E_K}{E_A}}$, E_A = diode voltage,

$$\sqrt{E_A}\sqrt{\frac{E_K}{E_A}} = M_{max}\sqrt{E_o}\,(.0336)$$

$$M_{max} = \sqrt{\frac{E_K}{E_o}}\,\frac{1}{.0336}$$

Oxide Cathode, $E_K = 0.1$ eV

Hence the maximum magnification does not depend on the diode voltage or spacing, but only on the initial voltage at the decelerator and the desired pencil angle.

The minimum magnification depends only on the choice of anode hole size.

When designed, M was chosen to be 1.13.

For Case 2 ~~initial and final image~~ the following system was tried, in analogy with condensing lenses in light optics:

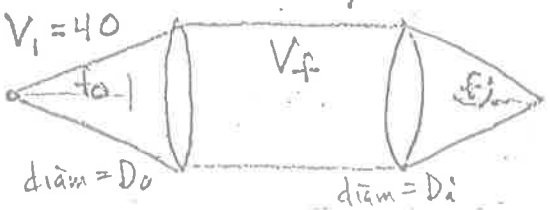

Assume that intermediate image between lenses is far to the right of L. Then from Newtonian lens equations (Lecture 2, p. ②):

$$M_1 = -\frac{L}{f_o\sqrt{\frac{V_f}{V_1}}} \qquad M_2 = \frac{f_i\sqrt{\frac{V_f}{V_2}}}{L}$$

$$M = M_1 M_2 = -\frac{f_i}{f_o}\sqrt{\frac{V_1}{V_2}}$$

To minimize space charge effects, operate with V_f more positive than $V_.$ To keep V_f down to a reasonable value, limit the ratio V_f/V_1 to 5. Then: $V_f/V_2 = 8$

$$f_o = 2.0\ D_o$$

$$f_i = 1.0\ D_i$$

$$M = 1.13 = \frac{f_i}{f_o}\sqrt{\frac{V_1}{V_2}} = .5\frac{D_i}{D_o}\sqrt{\frac{40}{25}} = .632\frac{D_i}{D_o}$$

So we have

$$\frac{D_i}{D_o} = 1.79$$

Angular magnification is $\frac{1}{M}\sqrt{\frac{V_1}{V_2}}$

$$= \frac{1.265}{1.13} = 1.12$$

System is now:

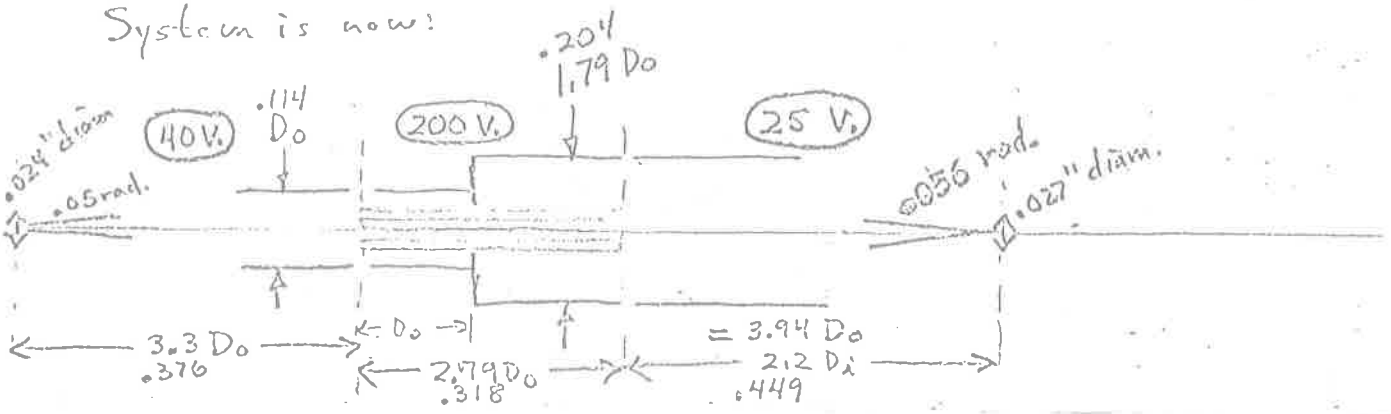

Beam size at first lens: $.024 + 2(.054 + .0178)3.3 D_o$

$= .024 + .447 D_o$

Beam size at second lens: $\geq .027 + 2(.056)3.94 D_o$

(larger, depending on beam angle) $= .027 + .441 D_o$

Assume beam size at first lens is $0.5 D_o$.

Then $.024 + .447 D_o = .5 D_o$

$.053 D_o = .024$

$D_o = .45$

Actual design has $D_o = .114$ (Was designed with small incident pencil angle, beam angle ignored.)

For this D_o, beam size at first lens is

$.024 + .447(.114) = .024 + .051 = .075$

"Filling factor" is $.075/.114 = .66$, and is satisfactory for use in a "condensor" lens.

Actual dimensions for $D_o = .114$ are on diagram on p. (8). The total length is $10.03 D_o = 1.143"$

To calculate beam size between the lenses, form the matrix for the first lens:

$$-\frac{1}{f_2}\begin{pmatrix} X_2 - F_2 & (X_1 - F_1)(X_2 - f_2) - f_1 f_2 \\ 1 & X_1 - F_1 \end{pmatrix} = -\frac{1}{.502}\begin{pmatrix} X_2 - .308 & -.228(.502) \\ 1 & 0 \end{pmatrix}$$

$$= \begin{pmatrix} -1.99X_2 + .614 & -.228 \\ -1.99 & 0 \end{pmatrix} \quad \text{For } X_2 = .114, \begin{pmatrix} .387 & -.228 \\ -1.99 & 0 \end{pmatrix}$$

$$\begin{pmatrix} .387 & -.228 \\ -1.99 & 0 \end{pmatrix}\begin{pmatrix} .012 \\ .0678 \end{pmatrix} = \begin{pmatrix} .0046 - .0155 \\ -.0239 \end{pmatrix} = \begin{pmatrix} -.0109 \\ -.0239 \end{pmatrix}$$

$$\begin{pmatrix} .387 & -.228 \\ -1.99 & 0 \end{pmatrix}\begin{pmatrix} .012 \\ -.0322 \end{pmatrix} = \begin{pmatrix} .0046 + .0075 \\ -.0239 \end{pmatrix} = \begin{pmatrix} .012 \\ -.0239 \end{pmatrix}$$

Hence aperture between lenses can be as small as .024" diam. without losing electrons.

The system is now completely designed. There remains the problem of locating the exit pupil so that we can find whether the apertures in the decelerator are filled.

$X_1 = 1.051 \quad X_2 = .318$

Matrix for first lens. $f_1 = .228 \quad f_2 = .502 \quad F_1 = .376 \quad F_2 = .308$

$$\mathfrak{M}_1 = -\frac{1}{.502}\begin{pmatrix} .01 & .675(.01) - .228(1.502) \\ 1 & .675 \end{pmatrix} = -\frac{1}{.502}\begin{pmatrix} .01 & -.1056 \\ 1 & .675 \end{pmatrix}$$

$X_1 = 0 \quad X_2$

Matrix for second lens $f_1 = .612 \quad f_2 = .204 \quad F_1 = .290 \quad F_2 = .444$

$$\mathfrak{M}_2 = -\frac{1}{.204}\begin{pmatrix} X_2 - .444 & -.290(X_2 - .444) - .1248 \\ 1 & -.290 \end{pmatrix} = -\frac{1}{.204}\begin{pmatrix} X_2 - .444 & -.290X_2 + .0039 \\ 1 & -.290 \end{pmatrix}$$

$$\mathfrak{M}_2\mathfrak{M}_1 = 9.77\begin{pmatrix} .01X_2 - .00444 - .290X_2 + .0039 & -.1056X_2 + .0469 - .1957X_2 + .00263 \\ .01 - .290 & -.1056 \quad -.1957 \end{pmatrix} = 9.77\begin{pmatrix} -.28X_2 - .00054 & -.3013X_2 + .0495 \\ -.28 & -.3013 \end{pmatrix} = \begin{pmatrix} -2.733X_2 - .00528 & -2.943X_2 + .484 \\ -2.733 & -2.943 \end{pmatrix}$$

Pupil is at $X_2 = \frac{.484}{2.943} = .164$

Magnification is $-.449 - .005 = -.454$

Radius of pupil is $|-.454| \times .034 = .0154 = r_p$

$r_w = .0135 \qquad z_p = -.285$

$\theta_p = \frac{.0154}{-.285} = -.0054 \qquad \theta_b = \frac{.0135}{-.285} = -.0047$

Corners of R-θ diagram at window are:

(.0135, -.0007)
(.0135, .0101)
(-.0135, .0007)
(-.0135, -.0101)

For the decelerator aperturing system:

$r_w = .0065$ $r_p = .0095$ $z_p = .278$

$\theta_p = \frac{.0095}{.278} = .00342$ $\theta_b = \frac{.0065}{1278} = .00234$

Corners of R-θ diagram at window are:

(.0065, .00108)
(.0065, -.00576)
(-.0065, -.00108)
(-.0065, .00576)

These R-θ diagrams are shown on p. (8). They show that a few per cent of the decelerator apertures is not filled by the electron beam.

Further calculations should be made to see if some other value of V_f would give an electron beam which would fill the decelerator apertures. Then Case I should be treated in the same way.

Electron Optics Lectures

Lecture 7

Chris E. Kuyatt

June 6, 1967

Properties of Spherical Deflector

[References will be made to Figures and Equations in C.E. Kuyatt and J. Arol Simpson, "Electron Monochromator Design", Rev. Sci. Instr. 38, 103 (1967)].

See Figure 3. With concentric hemispheres of radii $R_2 > R_1$, a $1/r^2$ electrostatic field is produced. Electrons enter near the center of the space between the spheres, and exit after being deflected by 180°. If $E_0 = eV_0$ is the energy in electron volts of electrons which travel in a circle of radius R_0, then the potential difference between the spheres is given by

$$V = V_0 \left(\frac{R_2}{R_1} - \frac{R_1}{R_2} \right)$$

The potential of the inner sphere is $V_0 \left(3 - \frac{2R_0}{R_1}\right)$ and of the outer sphere $V_0 \left(3 - \frac{2R_0}{R_2}\right)$. Dividing resistors to establish the mid-potential will in general be unequal.

Let x_1 be the radial distance of an incident electron measured from the path of radius R_0 and let α be the angle the incident electron makes with the path of radius R_0. Let x_2 be the radial distance of the outgoing electron measured from the

path of radius R_0. Then

$$\frac{X_2}{R_0} = -\frac{X_1}{R_0} + 2\frac{\Delta E}{E} + 2\alpha^2$$

where $\Delta E = E - E_0$. Note that the input plane is imaged onto the output plane with unity magnification. The absence of a term linear in α indicates first order angle focusing. The second term shows linear energy dispersion, and the last term gives the angular aberrations. (In the form $2R_0\alpha^2$ the last term is often called the trace width.)

Energy Resolution

To obtain the energy resolution, one must calculate the transmission of electrons as a function of energy, taking into account the distribution of the incident electrons over space and angle. With entrance and exit slits of equal width w (or with virtual slits), such a transmission function, neglecting the α^2 term, is a triangle with width at half height $\Delta E_{1/2}$ given by

$$\frac{\Delta E_{1/2}}{E_0} = \frac{W}{2R_0}$$

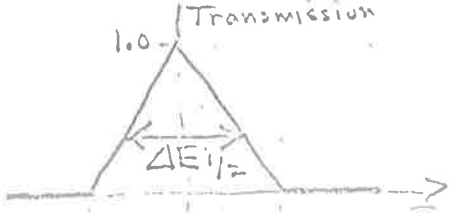

Use of a round entrance aperture would round and slightly narrow the transmission function:

I'll leave this narrowing as a small safety factor.

Addition of the α^2 term also has the effect of changing the shape of the transmission function without appreciably changing $\Delta E_{1/2}$ as long as $\alpha^2 < w/2R_0$. In fact, the change is less than 10% if $\alpha^2 = w/2R_0$. The base width of the transmission function is

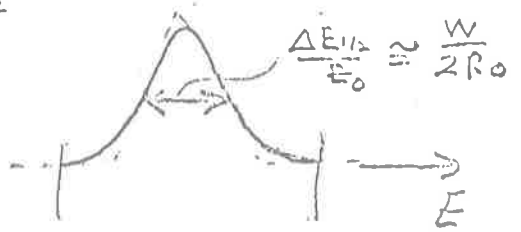

$$\frac{\Delta E_{base}}{E_0} = \frac{w}{R_0} + \alpha^2$$

To reduce the tailing of the line shape we have chosen

$$\alpha^2 = \frac{w}{4R_0} .$$

The base width is then

$$\frac{\Delta E_{base}}{E_0} \simeq 2.5 \frac{\Delta E_{1/2}}{E_0} \text{ s}$$

and

$$\frac{\Delta E_{1/2}}{E_0} \simeq \frac{w}{2R_0}$$

Maximum Width of Beam

A final property of the spherical deflector which we will need in our design work is the maximum deviation W_m from the central path:

$$\frac{W_m}{R_0} = \frac{\Delta E}{E_0} + \left[\alpha^2 + \left(\frac{W}{2R_0} + \frac{\Delta E}{E_0}\right)^2\right]^{1/2}$$

Note that for $w=0$, $\Delta E=0$, $W_m = R_0\alpha$.
In a typical case, $\frac{W}{2R_0} \ll 1$, $\frac{\Delta E}{E_0} \ll 1$, and the squared term is much smaller than α^2. Expanding,

$$\frac{W_m}{R_0} \cong \frac{\Delta E}{E_0} + \alpha + \frac{1}{2}\frac{\left(\frac{W}{2R_0} + \frac{\Delta E}{E_0}\right)^2}{\alpha}$$

The α term will give the major contribution.
[Example: $\frac{\Delta E_{1/2}}{E_0} = .01 = \frac{W}{2R_0}$, $\alpha^2 = .005$, $\frac{\Delta E}{E_0} = 1.25\frac{\Delta E_{1/2}}{E_0} = .0125$

$$\frac{W_m}{R_0} = .0125 + .071 + .0036 = .087$$

In our monochromator, $\left(\frac{W_m}{R_0}\right)_{max} = .125$]

Maximum $\Delta E_{1/2}$

Rewrite above equation:

$$\frac{W_m}{R_0} \cong 1.25\frac{\Delta E_{1/2}}{E_0} + \sqrt{\frac{1}{2}\frac{\Delta E_{1/2}}{E_0}} = 1.25\frac{\Delta E_{1/2}}{E_0} + .71\sqrt{\frac{\Delta E_{1/2}}{E_0}}$$

For a given spherical deflector, there is evidently a maximum value of $\Delta E_{1/2}$.

B. Internal Focusing Concentrated in Two Thin Lenses

[See Fig. 4(b)]

In this model space charge is considered only in the region between the slits and the thin lenses. The universal space charge curve is used to calculate the beam envelope. Calculations on this model show that the energy resolution is roughly constant up to a critical value of current and then increases rapidly. [See Fig. 5]. The critical current is

$$I_{crit} = 38.5\, E^{3/2} \alpha^2$$

C. Space Charge Lens Model

To a good approximation, space charge spreading can be considered to be the consequence of a negative lens in the region of minimum beam cross section, in particular at the entrance plane of the spherical deflector. If the electron beam is converging to a very small spot, after space charge spreading the beam appears to come from a very small spot. The critical current is the same as for model B above.

Optimum Monochromators

If we have chosen a value of $\Delta E_{1/2}$ and the size of the spherical deflector, only the electron energy E_0 at the spherical deflector remains to be chosen. The optimum value of E_0 depends on the space charge model we choose.

A. Monochromator with Real Apertures

This corresponds to space charge model B_0. We must take as the slit size the actual size of the space charge limited beam at the entrance plane of the spherical deflector. Otherwise current would be lost.

From Fig. 4(b), diameter of beam after space charge spreading is $\frac{1}{2}\pi R_0 \alpha$. Minimum beam diameter w is

$$w = \frac{\frac{1}{2}\pi R_0 \alpha}{2.35} \cong \frac{2}{3} R_0 \alpha$$

The basic monochromator eq's $\left[\frac{\Delta E_{1/2}}{E_0} = \frac{w}{2R_0},\ \alpha^2 = \frac{w}{4R_0}\right]$ then become

$$\frac{\Delta E_{1/2}}{E_0} = \frac{\alpha}{3} \quad \text{or} \quad 2\alpha^2 \quad \text{(whichever is greater)}.$$

The terms are equal when $\alpha = \frac{1}{6}$

For $\alpha < \frac{1}{6}$, $\alpha = 3\frac{\Delta E_{1/2}}{E_0}$

$$I_{total} = 38.5 E_0^{3/2} \alpha^2 \cong 350 E_0^{-1/2} (\Delta E_{1/2})^2$$

For $\alpha > \frac{1}{6}$, $\alpha^2 = \frac{1}{2}\frac{\Delta E_{1/2}}{E_0}$

$$I_{total} = 38.5 E_0^{3/2} \alpha^2 = 19.3 E_0^{1/2} \Delta E_{1/2}$$

For $\alpha = \frac{1}{6}$, $\frac{\Delta E_{1/2}}{E_0} = \frac{1}{18}$, $E_0 = 18\Delta E_{1/2}$

$$I_{total} = 38.5 E_0^{-3/2} \alpha^2 = 82 (\Delta E_{1/2})^{3/2}$$

To obtain monochromatized current, $I_{\Delta E}$, multiply I_{tot} by $\Delta E_{1/2} / \Delta E_K$ where ΔE_K is the effective energy width of the electron beam entering the monochromator. (For a thermionic cathode, $\Delta E_K \cong 2.5kT$)

$$I_{\Delta E} = 350 E_0^{-1/2} (\Delta E_{1/2})^3 / \Delta E_K \qquad E_0 \geq 18\Delta E_{1/2}$$

$$= 19.3 E_0^{1/2} (\Delta E_{1/2})^2 / \Delta E_K \qquad E_0 \leq 18\Delta E_{1/2}$$

OPTIMUM $\longrightarrow$ $= 82 (\Delta E_{1/2})^{5/2} / \Delta E_K \qquad E_0 = 18\Delta E_{1/2}$

These equations are plotted in Fig. 6, for $\Delta E_{1/2} = 0.02$ eV and $\Delta E_K = 0.25$ eV. Note that the optimum operation is predicted at

$$\frac{\Delta E_{1/2}}{E_0} = .0556,$$

a value too large for the hemispheres we use.

Operation at the maximum value of $\frac{\Delta E_{1/2}}{E_0}$ is predicted to give about ½ of the optimum current.

B. Monochromator with Virtual Apertures

In this case we can use the space charge lens model. By decelerating and/or magnifying the electron beam from a real aperture into the spherical deflector, the beam, after space charge spreading appears to come from a source of about the same size as would occur in the absence of space charge. The net result is to decouple the effective size of the electron beam (due to space charge spreading) from its angular divergence so one can choose an effective aperture size w. to satisfy

$$\frac{\Delta E_{1/2}}{E_0} = \frac{w}{2R_0}.$$

Then we can always choose $\alpha^2 = w^2/4R_0 = \frac{\Delta E}{2}$

Hence

$$I_{total} = 38.5\, E_0^{3/2} \alpha^2 = 19.3\, E_0^{1/2} \Delta E_{1/2}$$

The monochromatized current is then

$$I_{\Delta E} = 19.3\, E^{1/2} (\Delta E_{1/2})^2 / \Delta E_K$$

This equation is the same as the real slit equation for $E_o \leq 18.4 E^{1/2}$, but now there is no upper limit on E_o, and this model predicts that the amount of monochromatized current increases indefinitely as E_o is increased, while at the same time the effective aperture size w and entrance angle α must be reduced. This situation is shown by the dashed curve in Fig. 6.

Discuss anomalous energy spread.
Optimization with " " "

Show detailed sketch of apparatus.

Chris E. Kuyatt

June 20, 1967

Lecture 8

Analyzer Optimization

The problem is to optimize $l\,d\Omega$ at the scattering center while maintaining a given $\Delta E_{1/2}$ at the analyzer (spherical deflector). Space charge is negligible since currents are much lower than in the monochromator.

Scattering Geometry (Shown for 90° scattering)

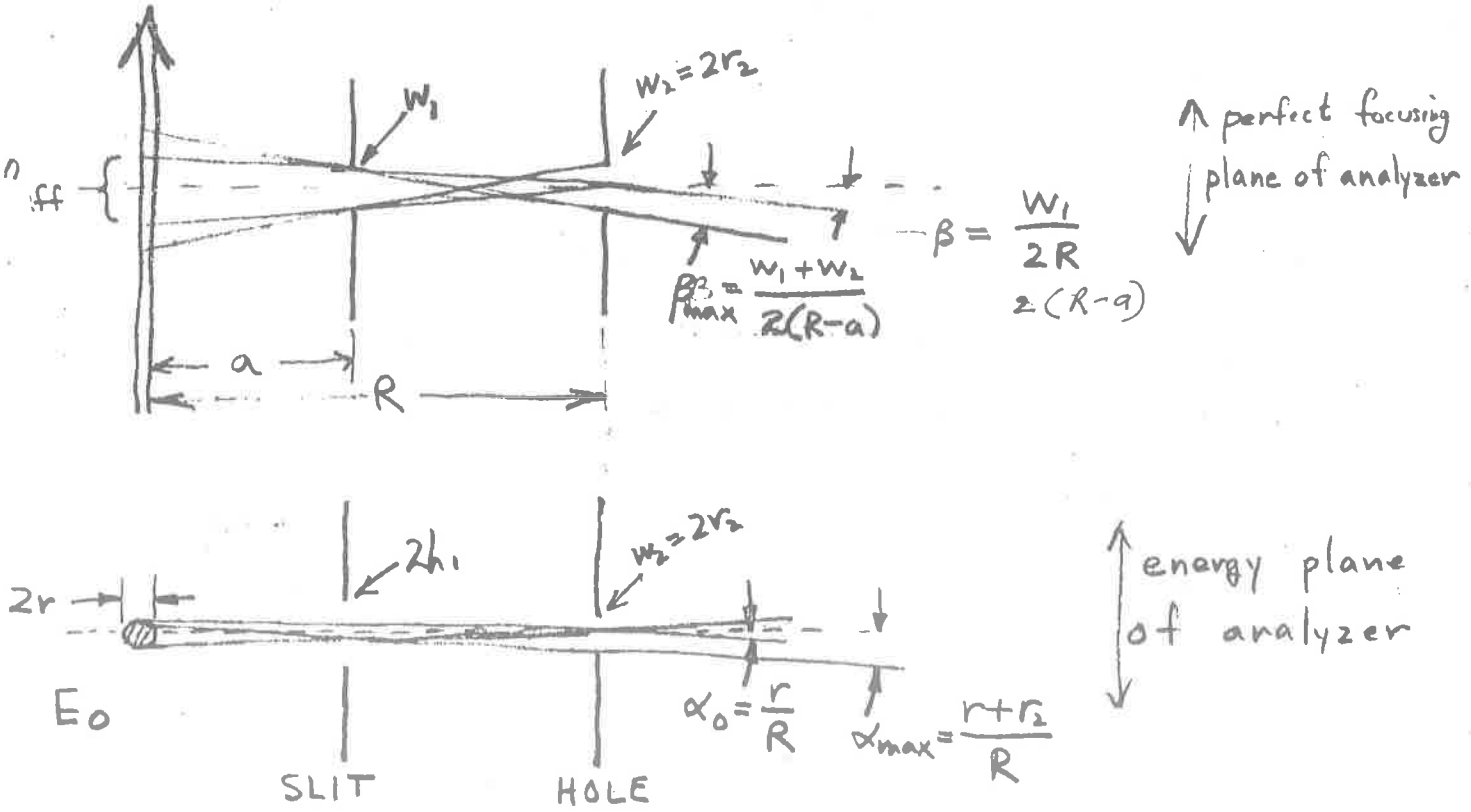

$$l_{eff} = W_1 \frac{R}{R-a} \qquad d\Omega_{eff} = \frac{\pi W_2^2}{4R^2}$$

$$(l\,d\Omega)_{eff} = \frac{\pi}{4} \frac{W_1 W_2^2}{R(R-a)}$$

Limitations on Magnification to Analyzer

Given w_2, α_0 at E_0 — scattering chamber

Let M_A = magnification to analyzer

E_A = analyzer energy

ΔE_A = resolution (full width at half-maximum)

w_A = width (diam) of beam at analyzer

r_A = mean radius of analyzer

From magnification,

$$w_A = M_A w_2 \qquad (1)$$

Helmholz-Lagrange gives

$$\sqrt{E_0}\, w_2 \alpha_0 = \sqrt{E_A}\, M_A w_2 \alpha_A$$

$$M_A = \sqrt{\frac{E_0}{E_A}}\, \frac{\alpha_0}{\alpha_A} \qquad (2)$$

To hold ΔE_A, we must restrict w_A and α_A:

$$w_A \leq 2 r_A \frac{\Delta E_A}{E_A} \qquad (3)$$

$$\alpha_A^2 \leq \frac{\Delta E_A}{2 E_A} \qquad (4)$$

From (1) and (3):

$$w_A = M_A w_2 \leq 2 r_A \frac{\Delta E_A}{E_A}$$

giving

$$M_A \leq 2 \frac{r_A}{w_2} \frac{\Delta E_A}{E_A} \qquad (5)$$

From (2) and (4):

$$\frac{\Delta E_A}{E_A} \geq 2\alpha_A^2 = \frac{2}{M_A^2}\,\frac{E_0}{E_A}\,\alpha_0^2$$

giving

$$M_A \geq \sqrt{\frac{2E_0}{\Delta E_A}}\,\alpha_0 \qquad (6)$$

Combining (5) and (6):

$$\boxed{\sqrt{\frac{2E_0}{\Delta E_A}}\,\alpha_0 \leq M_A \leq 2\,\frac{r_A}{w_2}\,\frac{\Delta E_A}{E_A}} \qquad (7)$$

Assuming that E_0 is given a maximum value, ΔE_A a minimum value, and that r_A is given a maximum value by mechanical considerations, the quantities α_0, w_2, and E_A remain at our disposal. They must satisfy (from Eq. (7)):

$$\boxed{\alpha_0 E_A w_2 \leq 2 r_A \Delta E_A \sqrt{\frac{\Delta E_A}{2E_0}}} \qquad (8)$$

If E_A could be made arbitrarily small, then $\alpha_0 w_2$ could be made arbitrarily large. However, there is a lower limit on the analyzing energy.

Lower Limit on Analyzing Energy

From Lecture 7, p. 5, to avoid filling the gap between the hemispheres, [For Gap/Radius = 1/4, and 80% filling factor]:

$$\frac{\Delta E_A}{E_A} \leq .01375 \,, \quad \alpha_A = \sqrt{\tfrac{1}{2}\frac{\Delta E_A}{E_A}} = .083 \text{ rad.}$$

So

$$E_A \geq \frac{\Delta E_A}{.01375} = 72.7\,\Delta E_A \qquad (9)$$

[If, for example, $\Delta E_A = .02$ eV, then $E_A \geq 1.454$ eV]

Putting (9) into (8), and using the equal signs in both equations

$$\boxed{\alpha_o W_2 = .0275\, r_A \sqrt{\frac{\Delta E_A}{2E_o}}} \qquad (10)$$

Note that $w_A = M_A w_2 = 2 r_A \frac{\Delta E_A}{E_A} = .0275\, r_A$

So that

$$\boxed{w_A = .0275\, r_A} \qquad (11)$$

For example, if $r_A = 1.0''$, $\Delta E_A = .02$ eV, $E_o = 400$ eV

$$\alpha_o W_2 = .0275\sqrt{\frac{.02}{800}} = .0001375 \text{ in-rad}$$

Optimum Scattering Geometry

We now have the maximum value of $\alpha_0 w_2$ given by Eq. (10). If the maximum beam diameter is $2r$, and the distance from beam to final hole is R, then the pencil angle at the hole is

$$\alpha_0 = \frac{r}{R} \qquad (11)$$

(Pencil angles are used because beam angle can be made zero at analyzer by use of a field lens.)

Substituting (11) in (10), and solving for w_2:

$$w_2 = .0275\, r_A \sqrt{\frac{\Delta E_A}{2E_0}}\, \frac{R}{r} \qquad (12)$$

and

$$M_A = \frac{w_A}{w_2} = \sqrt{\frac{2E_0}{\Delta E_A}}\, \frac{r}{R} \qquad (13)$$

Now assume that the pencil angle at the hole is the same in both planes. (It will turn out that the filling factor in the lens just before the analyzer will be large, and a larger angle in the perfect focusing plane will be difficult to handle.) Then it follows that, using Eq. (11)

$$l_{eff} = 2R\alpha_0 = 2r \qquad (14)$$

The quantity to be maximized is

$$\ell_{eff}\, d\Omega_{eff} = 2r \cdot \frac{\pi}{4} \frac{W_2^2}{R^2} \qquad (15)$$

Substituting (12) into (15):

$$(\ell\, d\Omega)_{eff} = \frac{\pi}{2} r\,(7.56\times10^{-4})\, r_A^2 \frac{\Delta E_A}{2E_0} \frac{1}{r^2}$$

$$= 5.94\times10^{-4} \frac{r_A^2}{r} \frac{\Delta E_A}{E_0} \qquad (16)$$

Hence $(\ell\, d\Omega)_{eff}$ can be made arbitrarily large by making r small and r_A large. Note that one gains faster by making r_A large than by making r small. Also, r small makes the beam angle $\frac{W_2}{2R}$ large.

In a practical system, a lower limit on r will be set in the beam forming system either by cathode loading or by difficulty in forming small apertures. An upper limit on r_A will be set by mechanical considerations such as room available or machining problems.

Note that Eq. (16) is independent of R. If R is decreased

M_A increases
W_2 decreases
α_0 increases (pencil angle)
$\frac{W_2}{2R}$ is constant (beam angle)

In our actual system, we chose

$r = .015''$

$R = 1.5''$

$\Delta E_A = .02$ eV

$E_0 = 200$ eV

$r_A = 1.0''$

Using our new equations

$w_A = .0275''$

$M_A = \sqrt{\frac{2 \times 200}{.02}} \frac{.015}{1.5} = 1.414$

$E_A = 1.454$ eV

$\alpha_A = .083$ rad.

$w_2 = \frac{w_A}{M_A} = .0195$

$(l d\Omega)_{eff} = \frac{5.94 \times 10^{-4}}{.015} \frac{.02}{200} = 3.96 \times 10^{-6}$ in-ster

$= 1.01 \times 10^{-5}$ cm-ster

$l_{eff} = .03'' = .075$ cm

$d\Omega_{eff} = 1.32 \times 10^{-4}$ ster.

$\alpha_0 = .01$ rad. (pencil angle)

$\frac{w_2}{2R} = \frac{.0195}{2 \times 1.5} = .0065$ rad. (beam angle)

The two angles are reasonably well-matched.

Finally, with $a = 0.5''$,

$w_1 = l_{eff} \frac{R-a}{R} = .03 \frac{1}{1.5} = .02''$

$2h_1 \geq .0265$

Actual Model B Design

Using slightly different design equations and assumptions (main difference was use of maximum angle rather than pencil angle):

$W_A = .030"$

$W_2 = .0144"$

$M_A = 2.09$

Same:
- $r = .015"$
- $R = 1.5"$
- $\Delta E_A = .02$ eV
- $E_o = 200$ eV
- $r_A = 1.0"$

$(\ell d\Omega)_{eff} = 1.10 \times 10^{-5}$ cm-ster

$\ell_{eff} = .06" \cong .15$ cm

$d\Omega_{eff} = 7.3 \times 10^{-5}$ ster

$E_A = 1.33$ eV

$\alpha_A = .048$ rad

(conservatively designed with maximum angle, not pencil angle)

$\alpha_o = .01$ rad. (pencil angle)

$\frac{W_2}{2R} = .0046$ rad. (beam angle)

$W_1 = .04"$ (gives pencil angle of .02 rad. in perfect focusing plane)

$2h_1 = .03"$

Since about Feb. 1967 we have been using

$W_1 = .02"$

$\ell_{eff} = .03"$

$(\ell d\Omega)_{eff} = .55 \times 10^{-5}$ cm-ster.

The pencil angle is the same in both planes.

Chris E. Kuyatt
June 23, 1967

Electron Lens Design, Scattering Chamber to Analyzer

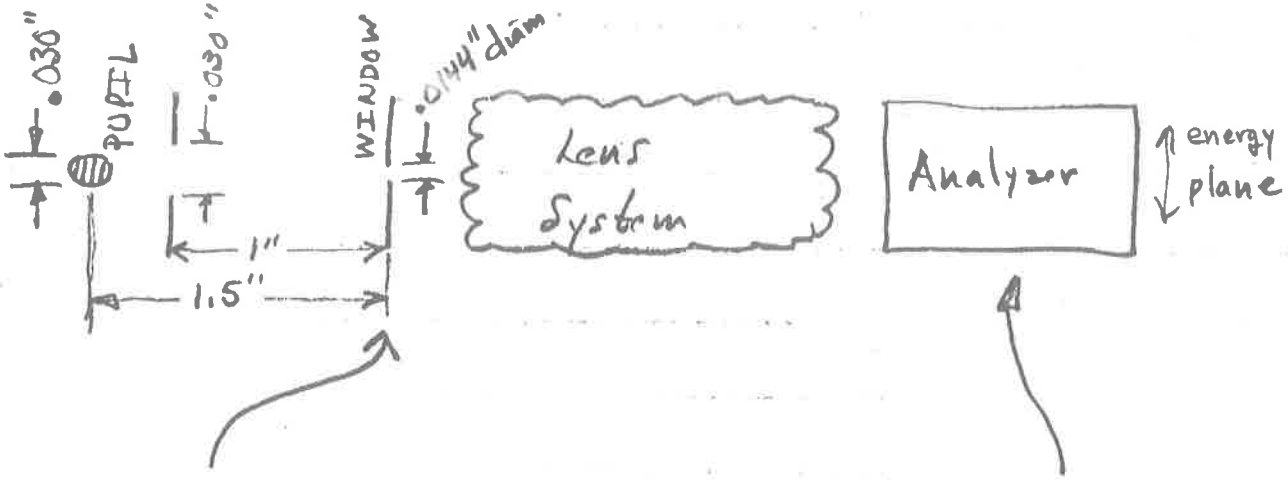

E_0 = 20eV to 200eV (and up)

α_0 = .01 rad. (pencil angle)
.02 rad. ($\perp$ plane)

W_2 = .0144" diam.

E_A = 1.33 or 3.33 eV

α_A = .048 rad. (energy plane)
.096 rad. ($\perp$ plane)

W_A = .030"

M_A = 2.09 (magnification from WINDOW to Analyzer entrance)

When Model B was actually designed, the maximum angle emerging from the scattering chamber was used, rather than the pencil angle. When transformed to the analyzer, α_A = .085 rad. in energy plane, .17 rad. in perpendicular plane. These large angles made the design of the final decelerator into the analyzer very difficult.

In arriving at a concept of the lens system, we note that the maximum deceleration ratio is 200/1.33 = 150. Such a large deceleration ratio can not be obtained in one stage, since the lens would be so strong that the image would be formed inside the lens field. Therefore, two stages of deceleration are needed, with a real image between them.

We decided to make the first deceleration stage variable, with the second stage into the analyzer having a fixed deceleration ratio:

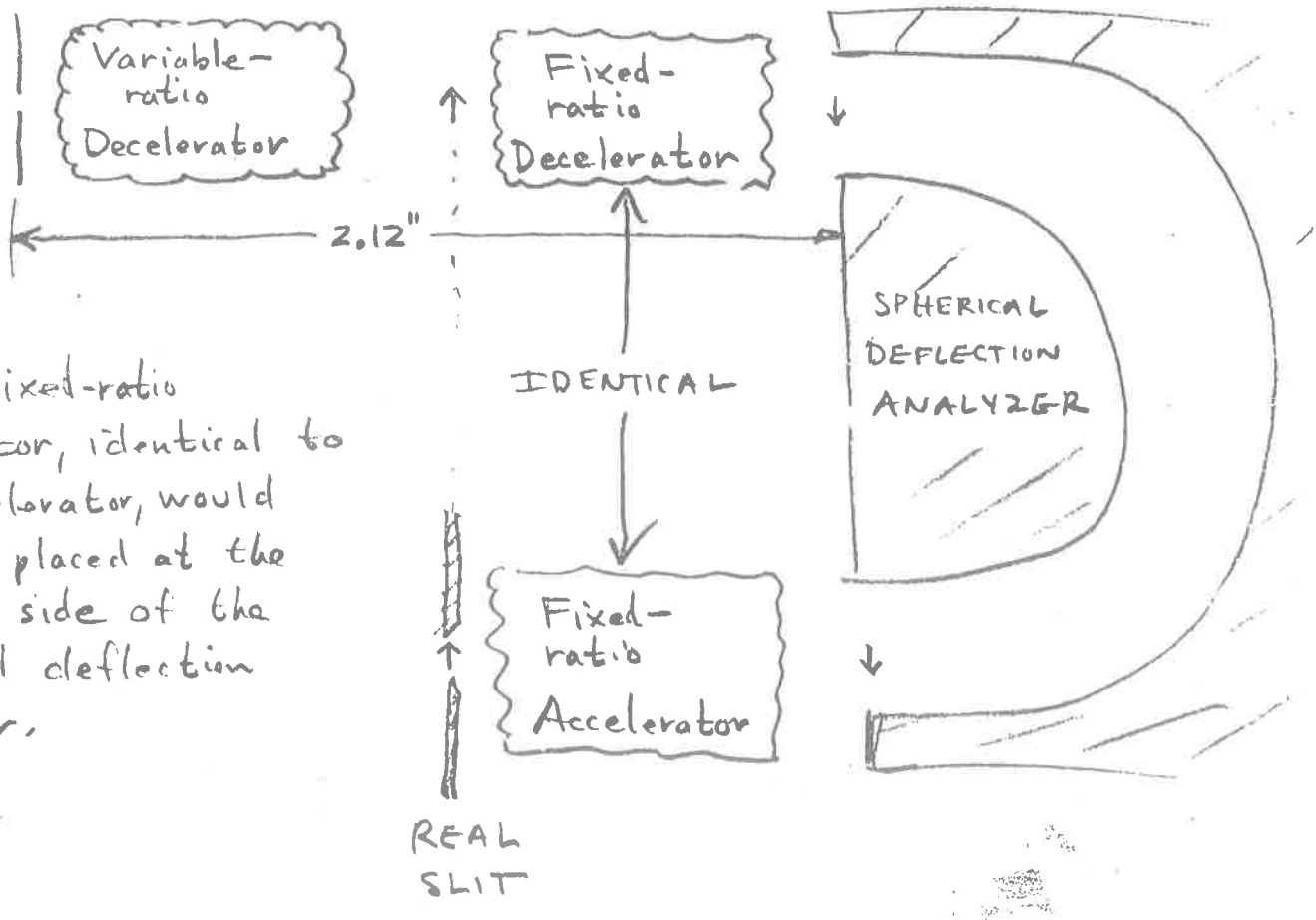

A fixed-ratio accelerator, identical to the decelerator, would then be placed at the output side of the spherical deflection analyzer.

Fixed-Ratio Decelerator

Use general method of design from Lecture 3, pp. 2 and 4.

Try 15:1 deceleration ratio

M = 1.5

$f_1 = .6\,D$ $F_1 = 1.7\,D$ $f_2 = 2.3\,D$ $F_2 = 0.9\,D$

low voltage high voltage

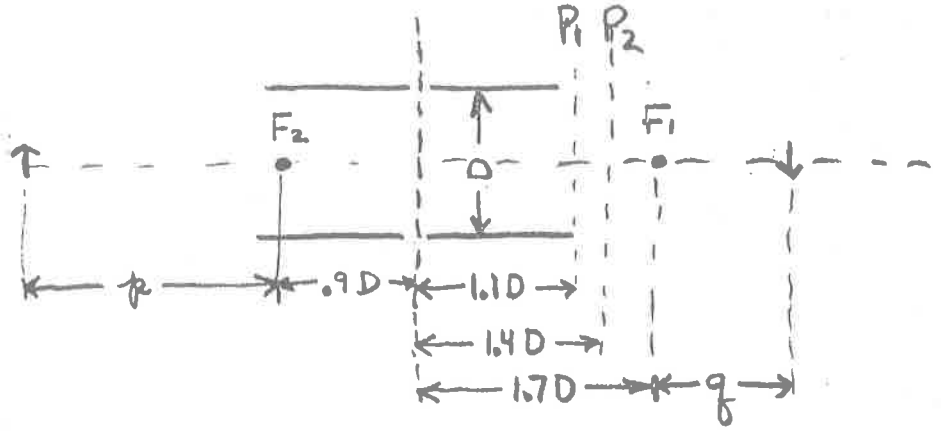

Final diameter .030"
Final pencil angle .17 rad.

Use thick lens equations

$p = f_2/M = 1.53\,D$

$q = Mf_1 = .9\,D$ Overall length = $5.03\,D$

Beam size on low voltage side:

$d \approx .030 + 2(.17)2.6D = .030 + .884\,D$

Filling factor

$\frac{d}{D} = \frac{.030}{D} + .884$ Too large

M = 1.0

$p = f_2/M = 2.3\,D$

$q = Mf_1 = .6\,D$ Overall length = $5.5\,D$

$d = .030 + 2(1.7)2.3D = .030 + .78\,D$

$\frac{d}{D} = \frac{.030}{D} + .78$ Still too large.

M=0.5 $p = f_2/M = 4.6\,D$

$q = Mf_1 = .3\,D$ Overall length = 7.5 D

$d \cong .030 + 2(.17)\,2.0\,D = .030 + .68\,D$

$\frac{d}{D} = \frac{.030}{D} + .68$ Still too large.

Making the magnification smaller will not help much. Hence a stronger lens is needed.

Try 26:1 deceleration ratio. Properties have to be estimated, since Spangenberg's data does not go to this large a ratio.

$f_1 \cong .35\,D$ $F_1 \cong 1.1\,D$ $f_2 \cong 1.75\,D$ $F_2 \cong .4\,D$

M=1

$p = f_2/M = 1.75\,D$

$q = Mf_1 = .35\,D$ Overall length = 3.6 D

$d \cong .030 + 2(.17)\,1.45\,D = .030 + .49\,D$

$\frac{d}{D} = \frac{.030}{D} + .49$ Getting close

M=0.5

$p = f_2/M = 3.5\,D$

$q = Mf_1 = .175\,D$ Overall length = 5.78 D

$d \cong .030 + 2(.17)\,1.275\,D = .030 + .43\,D$

$\frac{d}{D} = \frac{.030}{D} + .43$

With a reasonable D, filling factor can be held to about 50%.

A total length of 1.10" was available for this lens. Hence

$$D = \frac{1.1}{5.78} = .190"$$

and filling factor = .59

This filling factor is a little large, but since it is in the perfect focusing plane of the analyzer, the extra aberration blurring of the image is not crucial.

<u>As actually designed</u> for Model B,

$$D = .229" \quad M = 0.5$$

and the system is

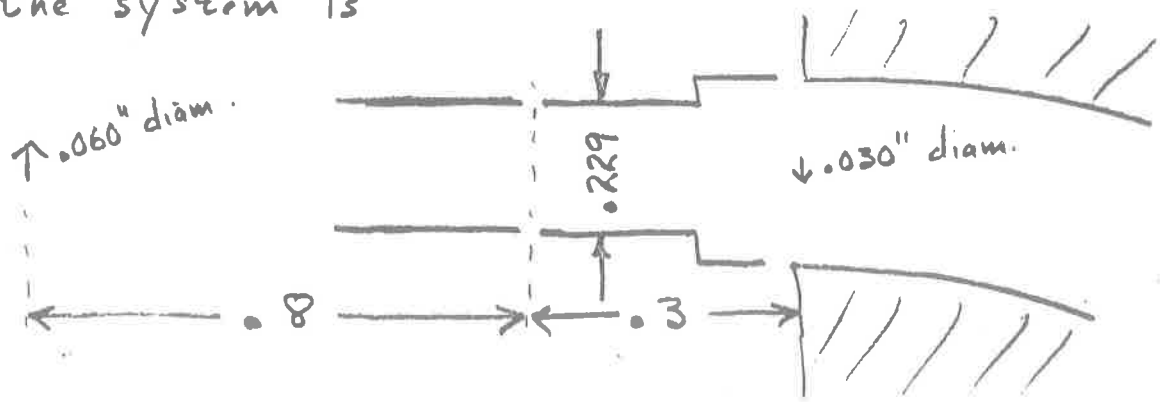

Note that the parameters of the actual system are not in good agreement with the above design data. This inconsistency arises because a different method of estimating the strong lens properties was used. It is likely that both estimates are in error, and that a precise design will only be possible when accurate lens data become available. In practice, the system is optimized by empirically finding the best voltage ratio for this lens.

We now know, however, that the beam angle can be made zero at the analyzer entrance plane (by using a field lens), leaving a maximum pencil angle of 0.096 rad, with a filling factor well under 50%. Also, a recent change in the slit system at the scattering chamber makes the pencil angle in the perfect focusing plane equal to the pencil angle in the energy plane, namely 0.048 rad. Therefore, the decelerating lens is very conservatively designed under present conditions.

With the present beam conditions, the decelerating lens could probably be redesigned for a lower voltage ratio, a shorter length, a higher magnification, or a combination of these properties.

Variable-Ratio "Decelerator"

$$\text{Magnification} = \frac{2.09}{.5} = 4.18$$

Deceleration Ratio: 5.77 maximum (200 : 34.6)
1.0 minimum

Acceleration Ratio: 1.0 minimum
4.33 maximum (20 : 86.6)

Available Length 1.02"

Using a three-tube lens (as in Lecture 3, pp. 5-7), the usual pattern will be to accelerate, then decelerate. Since for a single accelerating lens we have $M \cong 0.8 \frac{a}{p}$ (lecture 2, p. 6) and for a single decelerating lens $M \cong 1.25 \frac{a}{p}$, a closely spaced accelerating-decelerating combination will to a good approximation have $M \cong 1.0 \frac{a}{p}$.

For the present lens, $M \cong 4$, so $\frac{a}{p} \cong 4$. Hence we have:

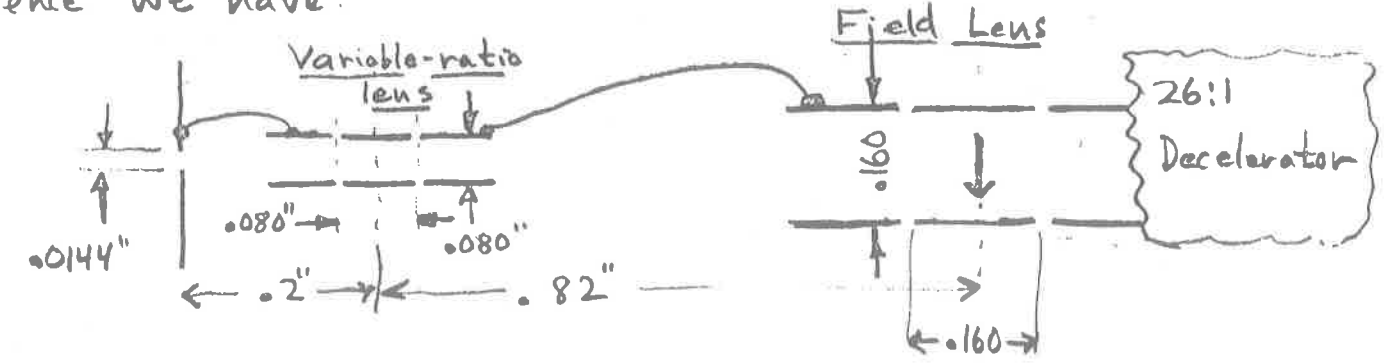

The incident beam has a maximum angle of .025 rad. Hence the approximate beam diameter at the variable-ratio lens is

$$.0144 + 2(.025).2 = .0244"$$

We decided to make the lens diameter .080" to leave room for misalinement and for beam expansion on the low energy side of the lens.

The computer program (Lecture 4) was used to calculate the properties of the entire analyzer input

system. As already discussed in Lecture 4, the final pupil of the system was found to be very close to the final window, leading to very large beam angles and a serious loss of electrons. The problem was solved by placing a three-tube einzel lens at the intermediate image. This lens functions as a field lens. It has very little effect on the overall imaging properties of the system, but gives excellent control over the final pupil position, and allows adjustment of the final beam angle to zero.

The field lens diameter was chosen by a trial-and-error process, using the computer program to decide whether good operation was possible over the entire range of operating conditions. The field lens diameter arrived at is .160". (See p. 7)

The final analyzer system is shown on the accompanying drawing. It includes the energy-add lens discussed in Lecture 4. The output leg of the analyzer is identical in function to the input leg. However, to transport the electron beam to a detector whose position was already fixed, the portion of the system <u>after</u> the analyzer exit slit was stretched a factor of 3. Because the output slit of the analyzer must be a real slit, the

field lens in the output leg of the analyzer had to be moved from its optimum position. A trial-and-error process was again used with the computer program to find an appropriate diameter for the lens which would give satisfactory operation over the entire range of operating conditions, and satisfy the additional requirement that it operate at the same voltage as the field lens in the input analyzer leg. The final configuration is shown on the drawing.

Use of the computer program enabled the operating voltages of the analyzer section to be calculated for a wide range of conditions. The results are shown on the next drawing. All voltages are given as ratios to the mid-voltage of the analyzer. (Experimentally, the mid-voltage is determined from the potential difference between the hemispheres, since contact potential effects tend to cancel out.)

Actual operating voltages on the field lenses agree well with the calculated values, but the variable-ratio lens in practice operates at a lower voltage than calculated, and the fixed-ratio decelerator gives best results when operated at a higher voltage ratio than calculated. (37:1). These disagreements have not yet been explained, but may possibly be

caused by inaccurate extrapolation of the lens characteristics to a voltage ratio of 26:1. If this extrapolation is in error it could easily lead to operating voltages different than those calculated. More accurate lens data must be obtained before this question can be settled.

The final drawing is a block diagram of the entire monochromator-analyzer system, with notations showing where in the Lectures each component is discussed.

The Future

Looking at the field of low-energy electron optics, as applied to the design of high-current guns, monochromators, and energy analyzers, I predict that the use of computers as an aid in the design process will increase markedly. The time is ripe for the development of computer programs which will ~~use relaxation techniques to~~ calculate potential distributions and electron trajectories in electron lenses and deflection analyzers to an accuracy in the range of 0.1 to 0.01 per cent. Some of the following will then be possible:

1) Calculation of precise focal properties for both simple and complicated lenses.
2) Calculation of aberration constants of electron lenses.
3) Tracing of skew rays through lenses.
4) Incorporation of the precise lens properties into computer programs which will calculate the properties of systems of several lenses to a few per cent.
5) Accurate treatment of the end effects (fringe fields) of deflection analyzers, leading to the development of terminating electrodes which will enable the analyzer to achieve its ideal characteristics.
6) The exploitation of new types of deflection analyzers (such as the cylindrical mirror of Zashkvara, et al Soviet Phys.-Tech. Phys. 11, 96 (1966)) will lead to monoenergetic

beams with much higher current, and to energy analyzers with a much larger solid angle, for the same energy resolution. By trading off current or solid angle, higher energy resolutions will become available.

7) Synthesis of electron optical elements of precisely known properties will lead to systems with accurately predictable properties. Such systems will be very valuable in the precise measurement of electron scattering.

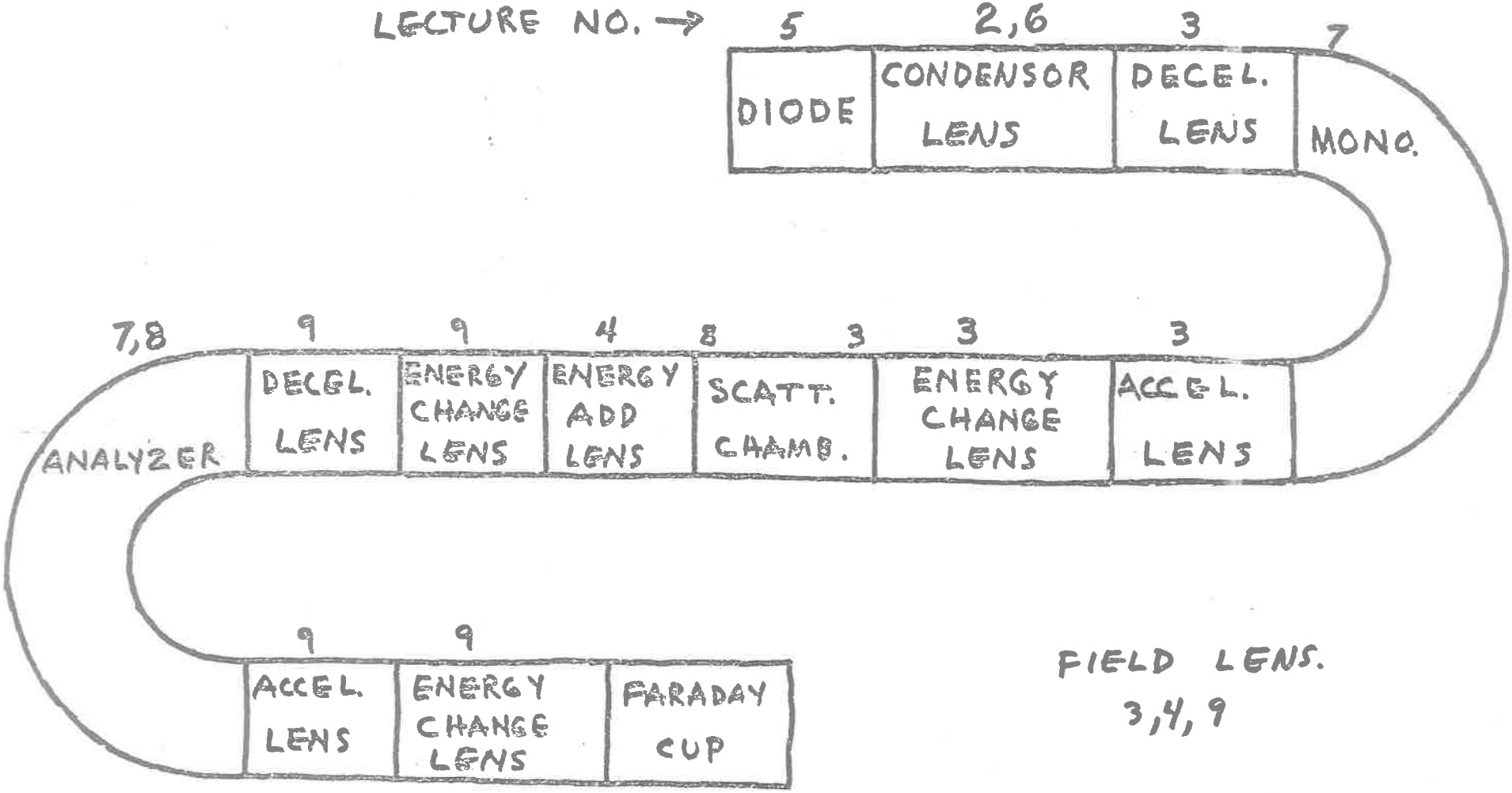
LECTURE NO. →
5
2,6
3
7
DIODE
CONDENSOR LENS
DECEL. LENS
MONO.
7,8
9
9
4
8
3
3
3
ANALYZER
DECEL. LENS
ENERGY CHANGE LENS
ENERGY ADD LENS
SCATT. CHAMB.
ENERGY CHANGE LENS
ACCEL. LENS
9
9
ACCEL. LENS
ENERGY CHANGE LENS
FARADAY CUP
FIELD LENS.
3,4,9

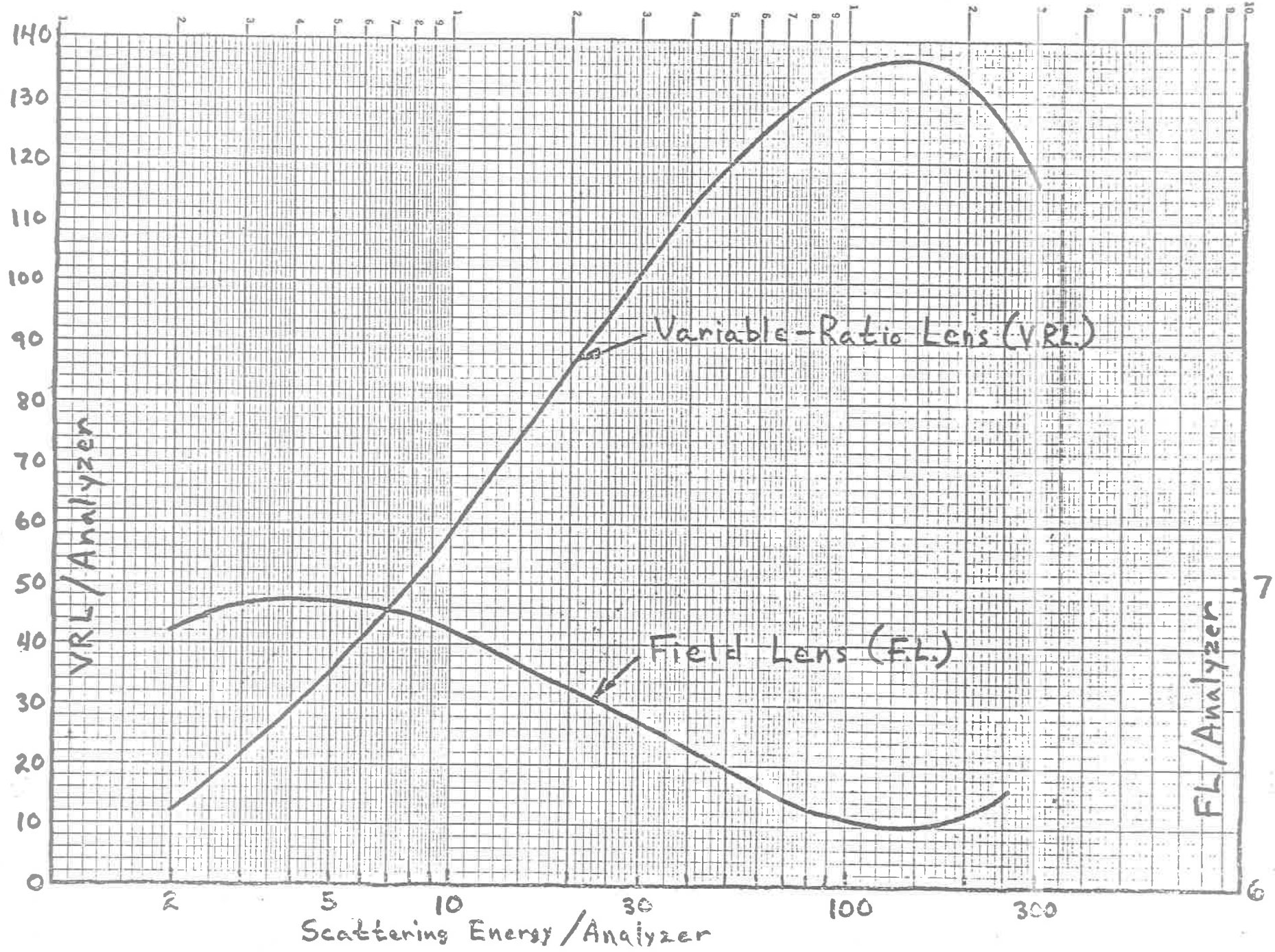
K&E SEMI-LOGARITHMIC
KEUFFEL & ESSER CO.
3 CYCLES X 70 DIVISIONS
359T-71G
MADE IN U.S.A.
ALBANENE
140
130
120
110
100
90
80
70
60
50
40
30
20
10
0
VRL/Analyzer
Variable-Ratio Lens (V.R.L.)
Field Lens (F.L.)
FL/Analyzer
7
6
2
5
10
30
100
300
Scattering Energy/Analyzer

Model B, Mark III (A2B) ANALYZER

June 1967

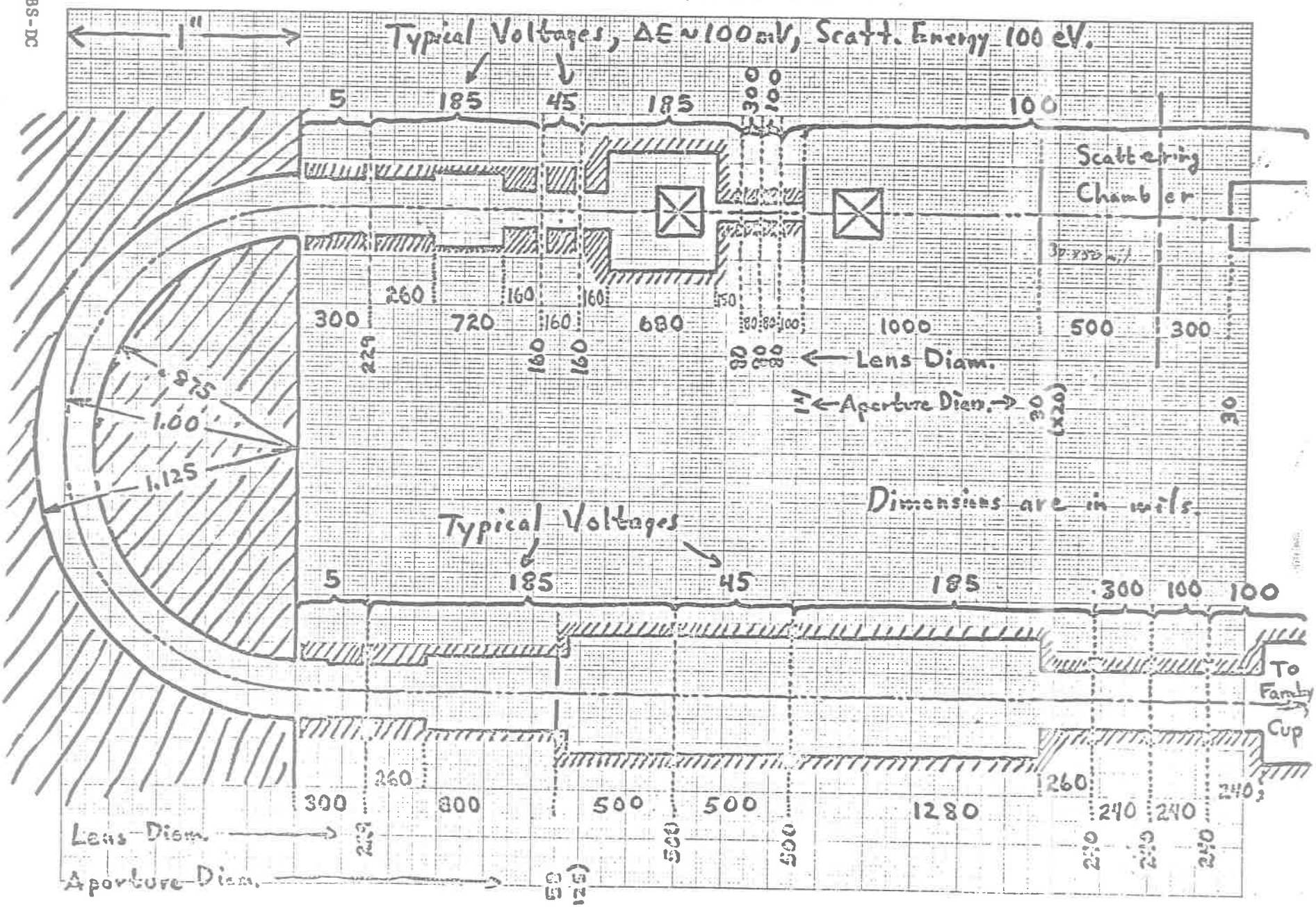

KEUFFEL & ESSER CO.

MONOCHROMATOR